arXiv:1609.00890v1 [math.CA] 4 Sep 2016

Hypercomplex Signal Energy Concentration in the Spatial and Quaternionic Linear Canonical Frequency Domains

Cuiming Zou[a], Kit Ian Kou[b,*]

[a]*Department of Mathematics, Faculty of Science and Technology, University of Macau, Taipa, Macao, China. Email: zoucuiming2006@163.com*
[b]*Department of Mathematics, Faculty of Science and Technology, University of Macau, Taipa, Macao, China.*

Abstract

Quaternionic Linear Canonical Transforms (QLCTs) are a family of integral transforms, which generalized the quaternionic Fourier transform and quaternionic fractional Fourier transform. In this paper, we extend the energy concentration problem for 2D hypercomplex signals (especially quaternionic signals). The most energy concentrated signals both in 2D spatial and quaternionic linear canonical frequency domains simultaneously are recently recognized to be the quaternionic prolate spheroidal wave functions (QPSWFs). The improved definitions of QPSWFs are studied which gave reasonable properties. The purpose of this paper is to understand the measurements of energy concentration in the 2D spatial and quaternionic linear canonical frequency domains. Examples of energy concentrated ratios between the truncated Gaussian function and QPSWFs intuitively illustrate that QPSWFs are more energy concentrated signals.

Keywords: Quaternionic linear canonical transforms, energy concentration, quaternionic Fourier transform, quaternionic prolate spheroidal wave functions.

*Corresponding author
Email address: kikou@umac.mo (Kit Ian Kou)

1. Introduction

The energy concentration problem in the time-frequency domain plays a crucial role in signal processing. The foundation of this problem comes from 1960s the research group of bell labs [1]. The problem states that for any given signal f with its Fourier transform (FT)

$$\mathcal{F}(f)(\omega) := \frac{1}{\sqrt{2\pi}} \int_{-\infty}^{\infty} f(t) e^{-\mathbf{i}\omega t} dt, \tag{1.1}$$

the energy ratios of the duration and bandwidth limiting of the signal f, i.e., $\alpha_f := \frac{\int_{-\tau}^{\tau} |f(t)|^2 dt}{\int_{-\infty}^{\infty} |f(t)|^2 dt}$ and $\beta_f := \frac{\int_{-\sigma}^{\sigma} |\mathcal{F}(f)(\omega)|^2 d\omega}{\int_{-\infty}^{\infty} |\mathcal{F}(f)(\omega)|^2 d\omega}$ of $f(t)$ both in fixed time $[-\tau, \tau]$ and frequency $[-\sigma, \sigma]$ domains, satisfy the following inequality

$$\arccos \alpha_f + \arccos \beta_f \geq \arccos \sqrt{\lambda_0}. \tag{1.2}$$

Let $E_f := \int_{-\infty}^{\infty} |f(t)|^2 dt$ be the total energy of f. By the Parseval theorem [2], the energy in time and frequency domains are equal, i.e., $E_f = E_{\mathcal{F}(f)}$. Without loss of generality, we consider the unit energy signals throughout this paper, i.e., $E_f = 1$.

The important constant λ_0 in Eq. (1.2) is the eigenvalue of the zero order prolate spheroidal wave functions (PSWFs). The PSWFs are originally used to solve the Helmhotz equation in prolate spheroidal coordinates by means of separation of variables [3, 4]. In 1960s, Slepian *et al.* [5, 6, 7] found that PSWFs are solutions for the energy concentration problem of bandlimited signals [2]. Their real-valued PSWFs are solutions of the integral equation

$$\int_{-\tau}^{\tau} f(x) \frac{\sin \sigma(x-y)}{\pi(x-y)} dx = \alpha f(y), \tag{1.3}$$

where α are eigenvalues of PSWFs. Here $[-\tau, \tau]$ and $[-\sigma, \sigma]$ are the fixed time and frequency domains, respectively. Important properties of PSWFs are given in [5, 8, 9, 10, 11]. The following properties follow form the general theory of integral equations and are stated without proof.

1. Eq.(1.3) has solutions only for real, positive values eigenvalues α_n. These values is a monotonically decreasing sequence, $1 > \alpha_0 > \alpha_1 > ... > \alpha_n > ... > 0$, such that $\lim_{n\to\infty} \alpha_n = 0$.
2. To each α_n there corresponds only one eigenfunction $\psi_n(x)$ with a constant factor. The functions $\{\psi_n(x)\}_{n=0}^{\infty}$ form a real orthonormal set in $\mathcal{L}^2([-\tau, \tau]; \mathbb{R})$.

3. An arbitrary real σ-bandlimited function $f(x)$ can be written as a sum

$$f(x) = \Sigma_{n=0}^{\infty} a_n \psi_n(x), \quad \text{for all } x \in \mathbb{R},$$

where $a_n := \int_{\mathbb{R}} f(x)\psi_n(x)dx$.

These properties are useful in solving the energy concentration problem and other applications [12, 13, 14, 15]. Slepian *et al.* [8] naturally extended them to higher dimension and discussed their approximation in some special case in the following years. After that, the works on this functions are slowly developed until 1980s a large number of engineering applied this functions to signal processing, such as bandlimited signals extrapolation, filter designing, reconstruction and so on [16, 17, 18].

The PSWFs have received intensive attention in recent years. There are many efforts to extend this kind of functions to various types of integral transformations. Pei *et al.* [12, 19] generalized PSWFs associated with the finite fractional Fourier transform (FrFT) and applied to the sampling theory. Zayed *et al.* [20, 21] generalized PSWFs not only associated with the finite FrFT but also associated with the linear canonical transforms (LCTs) and applied to sampling theory. Zhao *et al.* [13, 22] discussed the PSWFs associated with LCTs in detail and presented the maximally concentrated sequence in both time and LCTs-frequency domains. The wavelets based PSWFs constructed by Walter *et al.* [14, 15, 23] have some desirable properties lacking in other wavelet systems. Kou *et al.* [24] developed the PSWFs with noncommutative structures in Clifford algebra. They not only generalized the PSWFs in Clifford space (CPSWFs), but also extended the transform to Clifford LCT. But they just gave some basic properties of this functions and have not discussed details of the energy relationship for square integrable signals. In this paper, we consider the energy concentration problem for hypercomplex signals, especially for quaternionic signals [25, 26] associated with quaternionic LCTs (QLCTs) in detail. The improvement definition of QPSWFs are considered for odd and even quaternionic signals. The study is a great improvement on the one appeared in [24].

The QLCT is a generalization of the quaternionic FT (QFT) and quaternionic FrFT (QFrFT). The QFT and QFrFT are widely used for color image processing and signal analysis in these years [27, 28, 29, 30]. Therefore, it has more degrees of freedom than QFT and QFrFT, the performance will be more advanced in color image processing.

In the present paper, we generalize the 1D PSWFs under the QLCTs to the quaternion space, which are referred to as quaternionic PSWFs (QPSWFs). The

improved definition of QPSWFs associated with the QLCTs is studied and their some important properties are analyzed. In order to find the relationship of (α_f, β_f) for any square integrable quaternionic signal, we show that the Parseval theorem and studied the energy concentration problem associated with the QLCTs. In particularly, we utilize the quaternion-valued functions multiply two special chirp signals on both sides as a bridge between the QLCTs and the QFTs. The main goal of the present study is to develop the energy concentration problem associated with QLCTs. We find that the proposed QPSWFs are the most energy concentrated quaternionic signals.

The body of the present paper is organized as follows. In Section 2 and 3, some basic facts of quaternionic algebra and QLCTs are given. Moreover, the Parseval identity for quaternionic signals associated with the (two-sided) QLCTs are presented. In Section 4, the improved definition and some properties of QPSWFs associated with QLCTs are discussed. The Section 5 presents the main results, it includes two parts. In subsection 5.1, we introduce the existence theorem for the maximum energy concentrated bandlimited function on a fixed spatial domain associated with the QLCTs. In subsection 5.2, we discuss the energy extremal properties in fixed spatial and QLCTs-frequency domains for any quaternionic signal. In particular, we give an inequality to present the relationship of energy ratios for any quaternionic signal, which is analogue to the high dimensional real signals. Moreover, examples of energy concentrated ratios between the truncated Gaussian function and QPSWFs are presented, which can intuitively illustrate that QPSWFs are the more energy concentrated signals. Finally, some conclusion are drawn in Section 6.

2. Quaternionic Algebra

The present section collects some basic facts about quaternions [31, 32], which will be needed throughout the paper.

For all what follows, let $\mathbb{H}$ be the *Hamiltonian skew field of quaternions*:

$$\mathbb{H} := \{\boldsymbol{q} = q_0 + \mathbf{i}q_1 + \mathbf{j}q_2 + \mathbf{k}q_3 \,|\, q_0, q_1, q_2, q_3 \in \mathbb{R}\}, \tag{2.4}$$

which is an associative non-commutative four-dimensional algebra. The basis elements $\{\mathbf{i}, \mathbf{j}, \mathbf{k}\}$ obey the Hamilton's multiplication rules:

$$\mathbf{i}^2 = \mathbf{j}^2 = \mathbf{k}^2 = -1; \quad \mathbf{ij} = -\mathbf{ji} = \mathbf{k}, \ \mathbf{jk} = -\mathbf{kj} = \mathbf{i}, \ \mathbf{ki} = -\mathbf{ik} = \mathbf{j},$$

and the usual component-wise defined addition. In this way the quaternionic algebra arises as a natural extension of the complex field $\mathbb{C}$.

The *quaternion conjugate* of a quaternion $\boldsymbol{q}$ is defined by

$$\overline{\boldsymbol{q}} := q_0 - \mathbf{i}q_1 - \mathbf{j}q_2 - \mathbf{k}q_3, \quad q_0, q_1, q_2, q_3 \in \mathbb{R}.$$

We write $\mathbf{Sc}(\boldsymbol{q}) := \frac{1}{2}(\boldsymbol{q} + \overline{\boldsymbol{q}}) = q_0$ and $\mathbf{Vec}(\boldsymbol{q}) := \frac{1}{2}(q - \overline{q}) = \mathbf{i}q_1 + \mathbf{j}q_2 + \mathbf{k}q_3$, which are the *scalar* and *vector parts* of $\boldsymbol{q}$, respectively. This leads to a norm of $\boldsymbol{q} \in \mathbb{H}$ defined by

$$|\boldsymbol{q}| := \sqrt{\boldsymbol{q}\overline{\boldsymbol{q}}} = \sqrt{\overline{\boldsymbol{q}}\boldsymbol{q}} = (q_0^2 + q_1^2 + q_2^2 + q_3^2)^{\frac{1}{2}}.$$

Then we have $\overline{\boldsymbol{p}\boldsymbol{q}} = \overline{\boldsymbol{q}} \cdot \overline{\boldsymbol{p}}$, $|\boldsymbol{q}| = |\overline{\boldsymbol{q}}|$, $|\boldsymbol{p}\boldsymbol{q}| = |\boldsymbol{p}||\boldsymbol{q}|$, for any $\boldsymbol{p}, \boldsymbol{q} \in \mathbb{H}$. By (2.4), a quaternion-valued function or, briefly, an $\mathbb{H}$-valued function $\boldsymbol{f} : \mathbb{R}^2 \to \mathbb{H}$ can be expressed in the following form:

$$\boldsymbol{f}(x, y) = f_0(x, y) + \mathbf{i}f_1(x, y) + \mathbf{j}f_2(x, y) + \mathbf{k}f_3(x, y),$$

where $f_i : \mathbb{R}^2 \to \mathbb{R}$ $(i = 0, 1, 2, 3)$. For convenience's sake, in the considerations to follow we will rewrite $\boldsymbol{f}$ in the following symmetric form [33]:

$$\boldsymbol{f}(x, y) = f_0(x, y) + \mathbf{i}f_1(x, y) + f_2(x, y)\mathbf{j} + \mathbf{i}f_3(x, y)\mathbf{j}. \tag{2.5}$$

Properties (like integrability, continuity or differentiability) that are ascribed to $\boldsymbol{f}$ have to be fulfilled by all components f_i $(i = 0, 1, 2, 3)$.

In order to state our results, we shall need some further notations. The linear spaces $\mathcal{L}^p(\mathbb{R}^2; \mathbb{H})$ $(1 \leq p < \infty)$ consist of all $\mathbb{H}$-*valued functions* in $\mathbb{R}^2$ under left multiplication by quaternions, whose p-th power is Lebesgue integrable in $\mathbb{R}^2$:

$$\mathcal{L}^p(\mathbb{R}^2; \mathbb{H}) := \left\{ \boldsymbol{f} \;\middle|\; \boldsymbol{f} : \mathbb{R}^2 \to \mathbb{H},\ \|\boldsymbol{f}\|_{\mathcal{L}^p(\mathbb{R}^2;\mathbb{H})} := \left(\int_{\mathbb{R}^2} |\boldsymbol{f}(x, y)|^p dxdy \right)^{1/p} < \infty \right\}.$$

In this work, the *left* quaternionic inner product of $\boldsymbol{f}, \boldsymbol{g} \in \mathcal{L}^2(\mathbb{R}^2; \mathbb{H})$ is defined by

$$< \boldsymbol{f}, \boldsymbol{g} >_{\mathcal{L}^2(\mathbb{R}^2;\mathbb{H})} := \int_{\mathbb{R}^2} \boldsymbol{f}(x, y)\overline{\boldsymbol{g}(x, y)}dxdy. \tag{2.6}$$

The reader should note that the norm induced by the inner product (2.6),

$$\|\boldsymbol{f}\|^2 = \|\boldsymbol{f}\|^2_{\mathcal{L}^2(\mathbb{R}^2;\mathbb{H})} :=< \boldsymbol{f}, \boldsymbol{f} >_{\mathcal{L}^2(\mathbb{R}^2;\mathbb{H})} = \int_{\mathbb{R}^2} |\boldsymbol{f}(x, y)|^2 dxdy.$$

coincides with the $\mathcal{L}^2$-norm for $\boldsymbol{f}$, considered as a vector-valued function.

The angle between two non-zero functions $\boldsymbol{f}, \boldsymbol{g} \in \mathcal{L}^2(\mathbb{R}^2; \mathbb{H})$ is defined by

$$\arg(\boldsymbol{f}, \boldsymbol{g}) := \arccos\left(\frac{\mathbf{Sc}(< \boldsymbol{f}, \boldsymbol{g} >)}{\|\boldsymbol{f}\|\,\|\boldsymbol{g}\|} \right). \tag{2.7}$$

The superimposed argument is well-defined since, obviously, it holds

$$|\mathbf{Sc}(< \boldsymbol{f}, \boldsymbol{g} >)| \leq | < \boldsymbol{f}, \boldsymbol{g} >_{\mathcal{L}^2(\Omega;\mathbb{H})} | \leq \|\boldsymbol{f}\|\,\|\boldsymbol{g}\|.$$

3. The Quaternionic Linear Canonical Transforms (QLCTs)

The LCT was first proposed by Moshinsky and Collins [34, 35] in the 1970s. It is a linear integral transform, which includes many special cases, such as the Fourier transform (FT), the FrFT, the Fresnel transform, the Lorentz transform and scaling operations. In a way, the LCT has more degrees of freedom and is more flexible than the FT and the FrFT, but with similar computational costs as the conventional FT. Due to the mentioned advantages, it is of natural interest to extend the LCT to a quaternionic algebra framework. These extensions lead to the *Quaternionic Linear Canonical Transforms* (QLCTs). Due to the non-commutative property of multiplication of quaternions, there are different types of QLCTs. As explained in more detail below, we restrict our attention to the *two-sided* QLCTs [36, 37] of 2D quaternionic signals in this paper.

3.1. Definition of QLCTs Revisited

Definition 3.1 (Two-sided QLCTs) *Let* $A_i = \begin{pmatrix} a_i & b_i \\ c_i & d_i \end{pmatrix} \in \mathbb{R}^{2\times 2}$ *be a matrix parameter such that* $\det(A_i) = 1$, *for* $i = 1, 2$. *The two-sided QLCTs of signals* $\boldsymbol{f} \in \mathcal{L}^1 \bigcap \mathcal{L}^2(\mathbb{R}^2; \mathbb{H})$ *are given by*

$$\mathcal{L}(\boldsymbol{f})(u, v) := \int_{\mathbb{R}^2} K^{\mathbf{i}}_{A_1}(x, u)\boldsymbol{f}(x, y)K^{\mathbf{j}}_{A_2}(y, v)dxdy, \tag{3.8}$$

where the kernel functions are formulated by

$$K^{\mathbf{i}}_{A_1}(x, u) := \begin{cases} \frac{1}{\sqrt{\mathbf{i}2\pi b_1}} e^{\mathbf{i}\left(\frac{a_1}{2b_1}x^2 - \frac{1}{b_1}xu + \frac{d_1}{2b_1}u^2\right)}, & \text{for } b_1 \neq 0, \\ \sqrt{d_1}e^{\mathbf{i}(\frac{c_1 d_1}{2})u^2}, & \text{for } b_1 = 0, \end{cases} \tag{3.9}$$

and

$$K^{\mathbf{j}}_{A_2}(y, v) := \begin{cases} \frac{1}{\sqrt{\mathbf{j}2\pi b_2}} e^{\mathbf{j}\left(\frac{a_2}{2b_2}y^2 - \frac{1}{b_2}yv + \frac{d_2}{2b_2}v^2\right)}, & \text{for } b_2 \neq 0, \\ \sqrt{d_2}e^{\mathbf{j}(\frac{c_2 d_2}{2})v^2}, & \text{for } b_2 = 0. \end{cases} \tag{3.10}$$

It is significant to note that when $A_1 = A_2 = \begin{pmatrix} 0 & 1 \\ -1 & 0 \end{pmatrix}$, the QLCT of $\boldsymbol{f}$ reduces to $\frac{1}{\sqrt{\mathbf{i}2\pi}}\mathcal{F}(\boldsymbol{f})(u, v)\frac{1}{\sqrt{\mathbf{j}2\pi}}$, where

$$\mathcal{F}(\boldsymbol{f})(u, v) := \int_{\mathbb{R}^2} e^{-\mathbf{i}xu}\boldsymbol{f}(x, y)e^{-\mathbf{j}yv}dxdy \tag{3.11}$$

is the two-sided QFT of $\boldsymbol{f}$. Note that when $b_i = 0$ $(i = 1, 2)$, the QLCT of a signal is essentially a chirp multiplication and is of no particular interest for our objective interests. Without loss of generality, we set $b_i > 0$ $(i = 1, 2)$ throughout the paper.

Remark 3.1 *Let $b_1, b_2 \neq 0$. Using the Euler formula for the quaternionic linear canonical kernel we can rewrite Eq. (3.8) in the following form:*

$$\mathcal{L}(f)(u,v) = \frac{-\mathbf{i}\sqrt{\mathbf{i}}}{2\pi\sqrt{b_1 b_2}}\left(P_1 + \mathbf{i}P_2 + P_3\mathbf{j} + \mathbf{i}P_4\mathbf{j}\right)(-\mathbf{j}\sqrt{\mathbf{j}}),$$

where

$$\begin{aligned}
P_1 &:= \int_{\mathbb{R}^2} f(x,y)\cos\left(\frac{a_1}{2b_1}x^2 - \frac{1}{b_1}xu + \frac{d_1}{2b_1}u^2\right)\cos\left(\frac{a_2}{2b_2}y^2 - \frac{1}{b_2}yv + \frac{d_2}{2b_2}v^2\right)dxdy,\\
P_2 &:= \int_{\mathbb{R}^2} f(x,y)\sin\left(\frac{a_1}{2b_1}x^2 - \frac{1}{b_1}xu + \frac{d_1}{2b_1}u^2\right)\cos\left(\frac{a_2}{2b_2}y^2 - \frac{1}{b_2}yv + \frac{d_2}{2b_2}v^2\right)dxdy,\\
P_3 &:= \int_{\mathbb{R}^2} f(x,y)\cos\left(\frac{a_1}{2b_1}x^2 - \frac{1}{b_1}xu + \frac{d_1}{2b_1}u^2\right)\sin\left(\frac{a_2}{2b_2}y^2 - \frac{1}{b_2}yv + \frac{d_2}{2b_2}v^2\right)dxdy,\\
P_4 &:= \int_{\mathbb{R}^2} f(x,y)\sin\left(\frac{a_1}{2b_1}x^2 - \frac{1}{b_1}xu + \frac{d_1}{2b_1}u^2\right)\sin\left(\frac{a_2}{2b_2}y^2 - \frac{1}{b_2}yv + \frac{d_2}{2b_2}v^2\right)dxdy.
\end{aligned}$$

The above equation clearly shows how the QLCTs separate **real** *signals $f(x,y)$ into four quaternionic components, i.e., the even-even, odd-even, even-odd and odd-odd components of $f(x,y)$.*

From Eq. (3.8) if $\boldsymbol{f} \in \mathcal{L}^1 \bigcap \mathcal{L}^2(\mathbb{R}^2;\mathbb{H})$, then the two-sided QLCTs $\mathcal{L}(\boldsymbol{f})(u,v)$ has a symmetric representation

$$\mathcal{L}(\boldsymbol{f})(u,v) = \mathcal{L}(f_0)(u,v) + \mathcal{L}(f_1)(u,v)\mathbf{i} + \mathcal{L}(f_2)(u,v)\mathbf{j} + \mathbf{i}\mathcal{L}(f_3)(u,v)\mathbf{j},$$

where $\mathcal{L}(f_i)$ $(i = 0, 1, 2, 3)$ are the QLCTs of f_i and they are $\mathbb{H}$-valued functions.

Under suitable conditions, the inversion of two-sided quaternionic linear canonical transforms of $\boldsymbol{f}(u,v)$ can be defined as follows.

Definition 3.2 (Inversion QLCTs) *Suppose that $\boldsymbol{f} \in \mathcal{L}^1 \bigcap \mathcal{L}^2(\mathbb{R}^2,\mathbb{H})$. Then the inversion of two-sided QLCTs of $\boldsymbol{f}(u,v)$ are defined by*

$$\mathcal{L}^{-1}(\boldsymbol{f})(x,y) := \int_{\mathbb{R}^2} K^{\mathbf{i}}_{A_1^{-1}}(x,u)\boldsymbol{f}(u,v)K^{\mathbf{j}}_{A_2^{-1}}(y,v)dudv, \tag{3.12}$$

where $A_i^{-1} = \begin{pmatrix} d_i & -b_i \\ -c_i & a_i \end{pmatrix}$ *and* $\det(A_i^{-1}) = 1$ *for* $i = 1,\ 2$.

The following subsection describes the important relationship between QLCTs and QFT, which will be used to establish the main results in Section 5.

3.2. The Relation Between QLCTs and QFT

Note that the QLCTs of $\boldsymbol{f}$ multiple the chirp signals $2\pi\sqrt{b_1\mathbf{i}}e^{-\mathbf{i}\frac{d_1}{2b_1}u^2}$ on the left and $e^{-\mathbf{j}\frac{d_2}{2b_2}v^2}\sqrt{b_2\mathbf{j}}$ on the right can be regarded as the QFT on the scale domain. Since

$$\begin{aligned} & 2\pi\sqrt{b_1\mathbf{i}}e^{-\mathbf{i}\frac{d_1}{2b_1}u^2}\mathcal{L}(\boldsymbol{f})(u,v)e^{-\mathbf{j}\frac{d_2}{2b_2}v^2}\sqrt{b_2\mathbf{j}} \\ = & \int_{\mathbb{R}^2} e^{-\mathbf{i}\frac{1}{b_1}xu}\left(e^{\mathbf{i}\frac{a_1}{2b_1}x^2}\boldsymbol{f}(x,y)e^{\mathbf{j}\frac{a_2}{2b_2}y^2}\right)e^{-\mathbf{j}\frac{1}{b_2}yv}dxdy = \mathcal{F}(\tilde{\boldsymbol{f}})\left(\frac{u}{b_1},\frac{v}{b_2}\right), \end{aligned} \tag{3.13}$$

where $\tilde{\boldsymbol{f}}(x,y) := e^{\mathbf{i}\frac{a_1}{2b_1}x^2}\boldsymbol{f}(x,y)e^{\mathbf{j}\frac{a_2}{2b_2}y^2}$ is related to the parameter matrix $A_i,\ i=1,2$ in Eq. (3.8).

Lemma 3.1 (Relation Between QLCT and QFT) *Let* $A_i = \begin{pmatrix} a_i & b_i \\ c_i & d_i \end{pmatrix} \in \mathbb{R}^{2\times 2}$ *be a real matrix parameter such that* $\det(A_i) = 1$ *for* $i = 1,2$. *The relationship between two-sided QLCTs and QFTs of* $\boldsymbol{f} \in \mathcal{L}^1 \bigcap \mathcal{L}^2(\mathbb{R}^2;\mathbb{H})$ *are given by*

$$\mathcal{F}(\tilde{\boldsymbol{f}})\left(\frac{u}{b_1},\frac{v}{b_2}\right) = 2\pi\sqrt{b_1\mathbf{i}}e^{-\mathbf{i}\frac{d_1}{2b_1}u^2}\mathcal{L}(\boldsymbol{f})(u,v)e^{-\mathbf{j}\frac{d_2}{2b_2}v^2}\sqrt{b_2\mathbf{j}}, \tag{3.14}$$

where $\tilde{\boldsymbol{f}}(x,y) = e^{\mathbf{i}\frac{a_1}{2b_1}x^2}\boldsymbol{f}(x,y)e^{\mathbf{j}\frac{a_2}{2b_2}y^2}$.

3.3. Energy Theorem Associated with QLCTs

This subsection describes energy theorem of two-sided QLCTs [38], which will be applied to derive the extremal properties of QLCTs in Section 5.

Theorem 3.1 (Energy Theorem of the QLCTs) *Any 2D* $\mathbb{H}$*-valued function* $\boldsymbol{f} \in L^2(\mathbb{R}^2,\mathbb{H})$ *and its QLCT* $\mathcal{L}(\boldsymbol{f})$ *are related by the Parseval identity*

$$\|\boldsymbol{f}\|^2 = \|\mathcal{L}(\boldsymbol{f})\|^2. \tag{3.15}$$

Proof. For $\boldsymbol{f} \in L^2(\mathbb{R}^2,\mathbb{H})$, direct computation shows that

$$\|\mathcal{L}(\boldsymbol{f})\|^2 = \int_{\mathbb{R}^2}\mathcal{L}(\boldsymbol{f})(u,v)\overline{\mathcal{L}(\boldsymbol{f})(u,v)}dudv = \mathbf{Sc}\left[\int_{\mathbb{R}^2}\mathcal{L}(\boldsymbol{f})(u,v)\overline{\mathcal{L}(\boldsymbol{f})(u,v)}dudv\right].$$

Applying the definition of QLCTs, we have

$$\begin{aligned}
\|\mathcal{L}(\boldsymbol{f})\|^2 &= \mathbf{Sc}\left[\int_{\mathbb{R}^2}\left(\int_{\mathbb{R}^2} K^{\mathbf{i}}_{A_1}(x,u)\boldsymbol{f}(x,y)K^{\mathbf{j}}_{A_2}(y,v)dxdy\right)\overline{\mathcal{L}(\boldsymbol{f})(u,v)}dudv\right] \\
&= \mathbf{Sc}\left[\int_{\mathbb{R}^4} K^{\mathbf{i}}_{A_1}(x,u)\boldsymbol{f}(x,y)K^{\mathbf{j}}_{A_2}(y,v)\overline{\mathcal{L}(\boldsymbol{f})(u,v)}dxdydudv\right] \\
&= \int_{\mathbb{R}^4}\mathbf{Sc}\left[K^{\mathbf{i}}_{A_1}(x,u)\boldsymbol{f}(x,y)K^{\mathbf{j}}_{A_2}(y,v)\overline{\mathcal{L}(\boldsymbol{f})(u,v)}\right]dxdydudv.
\end{aligned}$$

With $\mathbf{Sc}(\boldsymbol{qp}) = \mathbf{Sc}(\boldsymbol{pq})$ for any $\boldsymbol{p},\boldsymbol{q}\in\mathbb{H}$ and $\overline{K^{\mathbf{i}}_{A_1}} = K^{\mathbf{i}}_{A_1^{-1}}$, $\overline{K^{\mathbf{j}}_{A_2}} = K^{\mathbf{j}}_{A_2^{-1}}$, we have

$$\begin{aligned}
\|\mathcal{L}(\boldsymbol{f})\|^2 &= \int_{\mathbb{R}^4}\mathbf{Sc}\left[\boldsymbol{f}(x,y)K^{\mathbf{j}}_{A_2}(y,v)\overline{\mathcal{L}(\boldsymbol{f})(u,v)}K^{\mathbf{i}}_{A_1}(x,u)\right]dxdydudv \\
&= \int_{\mathbb{R}^4}\mathbf{Sc}\left[\boldsymbol{f}(x,y)\overline{K^{\mathbf{i}}_{A_1^{-1}}(x,u)\mathcal{L}(\boldsymbol{f})(u,v)K^{\mathbf{j}}_{A_2^{-1}}(y,v)}\right]dxdydudv \\
&= \mathbf{Sc}\left[\int_{\mathbb{R}^2}\boldsymbol{f}(x,y)\overline{\int_{\mathbb{R}^2} K^{\mathbf{i}}_{A_1^{-1}}(x,u)\mathcal{L}(\boldsymbol{f})(u,v)K^{\mathbf{j}}_{A_2^{-1}}(y,v)dudv}dxdy\right] \\
&= \mathbf{Sc}\left[\int_{\mathbb{R}^2}\boldsymbol{f}(x,y)\overline{\boldsymbol{f}(x,y)}dxdy\right] = \int_{\mathbb{R}^2}\boldsymbol{f}(x,y)\overline{\boldsymbol{f}(x,y)}dxdy = \|\boldsymbol{f}\|^2.
\end{aligned}$$

Hence this completes the proof. □

Theorem 3.1 shows that the energy for an $\mathbb{H}$-valued signal in the spatial domain equals to the energy in the QLCTs-frequency domain. The Parseval theorem allows the energy of an $\mathbb{H}$-valued signal to be considered on either the spatial domain or the QLCTs-frequency domain, and exchange the domains for convenience computation.

Corollary 3.1 *The energy theorem of $\boldsymbol{f}$ and $\tilde{\boldsymbol{f}}(x,y) = e^{\mathbf{i}\frac{a_1}{2b_1}x^2}\boldsymbol{f}(x,y)e^{\mathbf{j}\frac{a_2}{2b_2}y^2}$ associated with their QFT is given by*

$$\|\boldsymbol{f}\|^2 = \|\tilde{\boldsymbol{f}}\|^2 = \|\mathcal{F}(\boldsymbol{f})\|^2. \tag{3.16}$$

4. The Quaternionic Prolate Spheroidal Wave Functions

In the following, we first explicitly present the definition of PSWFs associated with QLCTs.

4.1. Definitions of QPSWFs

Consider the 1D PSWFs [2, 5, 8, 24], let us extend the PSWFs to the quaternionic space associated with QLCTs.

Definition 4.1 (QPSWFs) *The solutions of the following integral equation in* $\mathcal{L}^1(\mathbb{R}^2;\mathbb{H})$

$$\lambda_n \mathbf{i}^{n-\frac{1}{2}}\psi_n(u,v)\mathbf{j}^{n-\frac{1}{2}} := \int_{\boldsymbol{\tau}} K^{\mathbf{i}}_{A_1'}(x,u)\psi_n(x,y)K^{\mathbf{j}}_{A_2'}(y,v)dxdy, \tag{4.17}$$

are called the quaternionic prolate spheroidal wave functions (QPSWFs) $\{\psi_n(x,y)\}_{n=0}^{\infty}$ *associated with QLCTs. Here, the complex valued* λ_n *are the eigenvalues corresponding to the eigenfunctions* $\psi_n(x,y)$*. The real parameter matrix* $A_i' := \begin{pmatrix} ca_i & b_i \\ cc_i & cd_i \end{pmatrix}$ *with* $a_id_i - b_ic_i = 1$*,* $b_i \neq 0$*, for* $i = 1, 2$*. The real constant* c *is a ratio about the frequency domain* $\boldsymbol{\sigma} := [-\sigma,\sigma]\times[-\sigma,\sigma]$ *and the spatial domain* $\boldsymbol{\tau} := [-\tau,\tau]\times[-\tau,\tau]$*, where* $c := \frac{\sigma}{\tau}$*,* $0 < c < \infty$*. Eq. (4.17) is named the finite QLCTs form of QPSWFs.*

Note that for simplicity of presentation, we write $\int_{-\tau}^{\tau}\int_{-\tau}^{\tau} = \int_{\boldsymbol{\tau}}$ and $\int_{-\sigma}^{\sigma}\int_{-\sigma}^{\sigma} = \int_{\boldsymbol{\sigma}}$.

Remark 4.1 *The solutions of this integral equation in Eq. (4.17) are well established in some special cases.*

(i) *In the square region* $\boldsymbol{\tau} = [-\tau,\tau]\times[-\tau,\tau]$*, if QLCTs are degenerated to 2D Fourier transform (FT), then QPSWFs becomes the 2D real PSWFs, which is given by*

$$\lambda_n\psi_n(u,v) = \int_{\boldsymbol{\tau}} e^{\mathbf{i}cxu}\psi_n(x,y)e^{\mathbf{i}cyv}dxdy.$$

Here, if $\psi_n(x,y)$ *is separable, i.e.,* $\psi_n(x,y) = \psi_n(x)\psi_n(y)$*, then the 2D PSWFs can be regarded as the product of two 1D PSWFs. To aid the reader, see [5] for more complete accounts of this subject.*

(ii) *In a unit disk, the QLCTs are degenerated to 2D FT, then the QPSWFs between the circular PSWFs [25]*

$$\lambda_n\psi_n(u,v) = \int_{x^2+y^2\leq 1} e^{\mathbf{i}(cxu+cyv)}\psi_n(x,y)dxdy.$$

Remark 4.2 *We call the right-hand side of Eq. (4.17) is the finite QLCTs. However,* $\det(A_i') = 1$*,* $i = 1, 2$ *only for the* $c = 1$*. There is a scale factor* c *added to the parameter matrix, which is different from the definition of QLCTs.*

4.2. Properties of QPSWFs

Some important properties of QPSWFs will be considered in this part, which are crucial in solving the energy concentration problem.

Proposition 4.1 (Low-pass Filtering Form in τ) *Let $\psi_n(x,y) \in \mathcal{L}^1(\mathbb{R}^2;\mathbb{H})$ be the QPSWFs associated with their QLCTs and $\tilde{\psi}(x,y) := e^{\mathbf{i}\frac{ca_1}{2b_1}x^2}\psi_n(x,y)e^{\mathbf{j}\frac{ca_2}{2b_2}y^2}$. Then $\{\tilde{\psi}_n(x,y)\}_{n=0}^{\infty}$ are solutions of the following integral equation*

$$\mu_n\tilde{\psi}_n(u,v) = \int_{\tau}\tilde{\psi}_n(x,y)\frac{\sin\sigma(x-u)}{\pi(x-u)}\frac{\sin\sigma(y-v)}{\pi(y-v)}dxdy, \tag{4.18}$$

where $\mu_n := c^4b_1b_2\lambda_n^2$ for $n = 0,1,2\cdots$ are the eigenvalues corresponding to $\tilde{\psi}_n(x,y)$ and $a_id_i - b_ic_i = 1$, $b_i \neq 0$, for $i = 1,2$, and $c := \frac{\sigma}{\tau}, 0 < c < \infty$. Eq. (4.18) is named the low-pass filtering form of QPSWFs associated with QLCTs.

Proof. We shall show that Eq. (4.18) is derived by the Eq. (4.17). Straightforward computations of the right-hand side of Eq. (4.18) show that

$$\begin{aligned}&\int_{\tau}\tilde{\psi}_n(x,y)\frac{\sin\sigma(x-u)}{\pi(x-u)}\frac{\sin\sigma(y-v)}{\pi(y-v)}dxdy\\ =\ &\int_{\tau}\frac{\sin\sigma(u-x)}{\pi(u-x)}e^{\mathbf{i}\frac{ca_1}{2b_1}x^2}\psi_n(x,y)e^{\mathbf{j}\frac{ca_2}{2b_2}y^2}\frac{\sin\sigma(v-y)}{\pi(v-y)}dxdy.\end{aligned}$$

Applying the following two important equations [39] to the last integral,

$$\frac{1}{2\pi}\int_{-\sigma}^{\sigma}e^{\mathbf{i}xu}dx = \frac{\sin(\sigma u)}{\pi u} \quad\text{and}\quad \frac{1}{2\pi}\int_{-\sigma}^{\sigma}e^{\mathbf{j}yv}dy = \frac{\sin(\sigma v)}{\pi v}, \tag{4.19}$$

then we have

$$\begin{aligned}&\int_{\tau}\frac{\sin\sigma(u-x)}{\pi(u-x)}e^{\mathbf{i}\frac{ca_1}{2b_1}x^2}\psi_n(x,y)e^{\mathbf{j}\frac{ca_2}{2b_2}y^2}\frac{\sin\sigma(v-y)}{\pi(v-y)}dxdy\\ =\ &\frac{1}{(2\pi)^2}\int_{\tau}\int_{\sigma}e^{\mathbf{i}v_1(u-x)}e^{\mathbf{i}\frac{ca_1}{2b_1}x^2}\psi_n(x,y)e^{\mathbf{j}\frac{ca_2}{2b_2}y^2}e^{\mathbf{j}v_2(v-y)}dv_1dv_2dxdy\\ =\ &\frac{1}{(2\pi)^2}\int_{\sigma}e^{\mathbf{i}v_1u}\left[\int_{\tau}e^{-\mathbf{i}\frac{cx}{b_1}(\frac{b_1v_1}{c})}e^{\mathbf{i}\frac{ca_1}{2b_1}x^2}\psi_n(x,y)e^{\mathbf{j}\frac{ca_2}{2b_2}y^2}e^{-\mathbf{j}\frac{cy}{b_2}(\frac{b_2v_2}{c})}dxdy\right]e^{\mathbf{j}v_2v}dv_1dv_2.\end{aligned}$$

Combining Eq.(4.17) with the parameter matrices $A_i' = \begin{pmatrix} ca_i & b_i \\ cc_i & cd_i \end{pmatrix}, i = 1,2$, and

$A_i' = \begin{pmatrix} -cd_ib_i^2 & b_i \\ cc_i & -\frac{ca_i}{b_i^2} \end{pmatrix}, i = 1, 2$, we have

$$
\begin{aligned}
& \frac{1}{(2\pi)^2}\int_{\boldsymbol{\sigma}} e^{\mathbf{i}v_1u}\left[\int_{\boldsymbol{\tau}} e^{-\mathbf{i}\frac{cx}{b_1}(\frac{b_1v_1}{c})} e^{\mathbf{i}\frac{ca_1}{2b_1}x^2}\boldsymbol{\psi}_n(x,y)e^{\mathbf{j}\frac{ca_2}{2b_2}y^2} e^{-\mathbf{j}\frac{cy}{b_2}(\frac{b_2v_2}{c})}dxdy\right]e^{\mathbf{j}v_2v}dv_1dv_2 \\
= & \frac{1}{2\pi}\int_{\boldsymbol{\sigma}} e^{\mathbf{i}v_1u}\left[\lambda_n e^{-\mathbf{i}\frac{cd_1}{2b_1}(\frac{b_1v_1}{c})^2}\mathbf{i}^n\sqrt{cb_1}\boldsymbol{\psi}_n\Big(\frac{b_1v_1}{cb_1},\frac{b_2v_2}{cb_2}\Big)\sqrt{cb_2}\mathbf{j}^n e^{-\mathbf{j}\frac{cd_2}{2b_2}(\frac{b_2v_2}{c})^2}\right]e^{\mathbf{j}v_2v}dv_1dv_2 \\
= & \frac{1}{2\pi}\lambda_n\int_{\boldsymbol{\sigma}} e^{\mathbf{i}v_1u}\left[e^{-\mathbf{i}\frac{cd_1b_1}{2}(\frac{v_1}{c})^2}\mathbf{i}^n\sqrt{cb_1}\boldsymbol{\psi}_n\Big(\frac{v_1}{c},\frac{v_2}{c}\Big)\sqrt{cb_2}\mathbf{j}^n e^{-\mathbf{j}\frac{cd_2b_2}{2}(\frac{v_2}{c})^2}\right]e^{\mathbf{j}v_2v}dv_1dv_2 \\
= & \frac{1}{2\pi}\lambda_n c^3\sqrt{b_1b_2}\mathbf{i}^n\left[\int_{\boldsymbol{\tau}} e^{\mathbf{i}w_1cu}e^{-\mathbf{i}\frac{cd_1b_1}{2}w_1^2}\boldsymbol{\psi}_n(w_1,w_2)e^{-\mathbf{j}\frac{cd_2b_2}{2}w_2^2}e^{\mathbf{j}w_2cv}dw_1dw_2\right]\mathbf{j}^n \\
= & \lambda_n c^3\sqrt{b_1b_2}\mathbf{i}^n\left[\lambda_n e^{-\mathbf{i}\frac{c(\frac{-a_1}{b_1^2})}{2b_1}(ub_1)^2}\frac{(-\mathbf{i})^n}{\sqrt{\mathbf{i}}}\sqrt{cb_1\mathbf{i}}\boldsymbol{\psi}_n\Big(\frac{ub_1}{b_1},\frac{vb_2}{b_2}\Big)\sqrt{cb_2\mathbf{j}}\frac{(-\mathbf{j})^n}{\sqrt{\mathbf{j}}}e^{-\mathbf{j}\frac{c(\frac{-a_2}{b_2^2})}{2b_2}(vb_2)^2}\right]\mathbf{j}^n \\
= & \lambda_n^2c^4b_1b_2e^{\mathbf{i}\frac{ca_1}{2b_1}u^2}\boldsymbol{\psi}_n(u,v)e^{\mathbf{j}\frac{ca_2}{2b_2}v^2} = c^4b_1b_2\lambda_n^2\tilde{\boldsymbol{\psi}}_n(u,v) =: \mu_n\tilde{\boldsymbol{\psi}}_n(u,v).
\end{aligned}
$$

The proof is complete. □

Remark 4.3 *For the specific parameters $a_i = 0, b_i = 1, c_i = -1, d_i = 0, i = 1, 2$, Eq. (4.18) becomes the low-pass form of QPSWFs associated with QFT*

$$\int_{\boldsymbol{\tau}}\boldsymbol{\psi}_n(x,y)\frac{\sin\sigma(x-u)}{\pi(x-u)}\frac{\sin\sigma(y-v)}{\pi(y-v)}dxdy = c^2\lambda_n^2\boldsymbol{\psi}_n(u,v).$$

To obtain the following property, we shall show a special convolution theorem of any $\mathbb{H}$-valued signal and real-valued signal.

Lemma 4.1 *Let $\boldsymbol{f} \in \mathcal{L}^1(\mathbb{R}^2;\mathbb{H})$ and $g \in \mathcal{L}^1(\mathbb{R}^2;\mathbb{R})$ associated with their QFT $\mathcal{F}(\boldsymbol{f})$ and $\mathcal{F}(g)$ with $\boldsymbol{f} = f_0 + \mathbf{i}f_1 + f_2\mathbf{j} + \mathbf{i}f_3\mathbf{j}$, where $f_i \in \mathcal{L}^1(\mathbb{R}^2;\mathbb{R})$, $i = 0, 1, 2, 3$ and $\mathcal{F}(g) \in \mathcal{L}^1(\mathbb{R}^2;\mathbb{R})$. The convolution of $\boldsymbol{f}$ and g is defined as*

$$(\boldsymbol{f} * g)(s,t) := \int_{\mathbb{R}^2}\boldsymbol{f}(x,y)g(s-x,t-y)dxdy. \tag{4.20}$$

Then the QFT for $\boldsymbol{f} * g$ holds

$$
\begin{aligned}
& \mathcal{F}\left(\boldsymbol{f} * g\right)(u,v) \\
= & \mathcal{F}(f_0 + \mathbf{i}f_1)(u,v)\mathcal{F}(g)(u,v) + \mathcal{F}(f_2\mathbf{j} + \mathbf{i}f_3\mathbf{j})(u,v)\mathcal{F}(g)(-u,v).
\end{aligned} \tag{4.21}
$$

Proof. Let $s - x = m$ and $t - y = n$, straightforward computation the QFT in Eq.(3.11) of the convolution between f and g shows that

$$\begin{aligned}
&\mathcal{F}\left(\int_{\mathbb{R}^2} \boldsymbol{f}(x,y)g(s-x,t-y)dxdy\right)(u,v)\\
=\ &\int_{\mathbb{R}^2} e^{-\mathbf{i}su}\left(\int_{\mathbb{R}^2} \boldsymbol{f}(x,y)g(s-x,t-y)dxdy\right)e^{-\mathbf{j}tv}dsdt\\
=\ &\int_{\mathbb{R}^2} e^{-\mathbf{i}(x+m)u}\left(\int_{\mathbb{R}^2} \boldsymbol{f}(x,y)g(m,n)dxdy\right)e^{-\mathbf{j}(y+n)v}dmdn\\
=\ &\int_{\mathbb{R}^4} e^{-\mathbf{i}mu}e^{-\mathbf{i}xu}\left[(f_0(x,y)+\mathbf{i}f_1(x,y))+(f_2(x,y)\mathbf{j}+\mathbf{i}f_3(x,y)\mathbf{j})\right]g(m,n)e^{-\mathbf{j}yv}e^{-\mathbf{j}nv}dxdydmdn.
\end{aligned}$$

With $e^{-\mathbf{i}}\mathbf{j} = \mathbf{j}e^{\mathbf{i}}$, the last integral becomes

$$\begin{aligned}
&\int_{\mathbb{R}^4} e^{-\mathbf{i}xu}\left(f_0(x,y)+\mathbf{i}f_1(x,y)\right)e^{-\mathbf{i}mu}g(m,n)e^{-\mathbf{j}nv}e^{-\mathbf{j}yv}dxdydmdn\\
+\ &\int_{\mathbb{R}^4} e^{-\mathbf{i}xu}\left(f_2(x,y)\mathbf{j}+\mathbf{i}f_3(x,y)\mathbf{j}\right)e^{\mathbf{i}mu}g(m,n)e^{-\mathbf{j}nv}e^{-\mathbf{j}yv}dxdydmdn\\
=\ &\int_{\mathbb{R}^2} e^{-\mathbf{i}xu}\left(f_0(x,y)+\mathbf{i}f_1(x,y)\right)\mathcal{F}(g)(u,v)e^{-\mathbf{j}yv}dxdy\\
+\ &\int_{\mathbb{R}^2} e^{-\mathbf{i}xu}\left(f_2(x,y)\mathbf{j}+\mathbf{i}f_3(x,y)\mathbf{j}\right)\mathcal{F}(g)(-u,v)e^{-\mathbf{j}yv}dxdy.
\end{aligned}$$

Since we have known $\mathcal{F}(g)$ is real-valued, then we have

$$\begin{aligned}
&\int_{\mathbb{R}^2} e^{-\mathbf{i}xu}\left(f_0(x,y)+\mathbf{i}f_1(x,y)\right)e^{-\mathbf{j}yv}\mathcal{F}(g)(u,v)dxdy\\
+\ &\int_{\mathbb{R}^2} e^{-\mathbf{i}xu}\left(f_2(x,y)\mathbf{j}+\mathbf{i}f_3(x,y)\mathbf{j}\right)e^{-\mathbf{j}yv}\mathcal{F}(g)(-u,v)dxdy\\
=\ &\mathcal{F}(f_0)(u,v)\mathcal{F}(g)(u,v)+\mathbf{i}\mathcal{F}(f_1)(u,v)\mathcal{F}(g)(u,v)\\
+\ &\mathcal{F}(f_2)(u,v)\mathcal{F}(g)(-u,v)\mathbf{j}+\mathbf{i}\mathcal{F}(f_3\mathbf{j})(u,v)\mathcal{F}(g)(-u,v).
\end{aligned}$$

This completes the proof. □

Note that if the real signal $g(x,y) = g(-x,y)$ with $\mathcal{F}(g)$ is real valued, then $\mathcal{F}(g)(u,v) = \mathcal{F}(g)(-u,v)$. It means that

$$\begin{aligned}
&\mathcal{F}\left(\boldsymbol{f} * g\right)(u,v)\\
=\ &\mathcal{F}(f_0+\mathbf{i}f_1)(u,v)\mathcal{F}(g)(u,v)+\mathcal{F}(f_2\mathbf{j}+\mathbf{i}f_3\mathbf{j})(u,v)\mathcal{F}(g)(-u,v)\\
=\ &\mathcal{F}(f_0+\mathbf{i}f_1+f^2\mathbf{j}+\mathbf{i}f_3\mathbf{j})(u,v)\mathcal{F}(g)(u,v)\\
=\ &\mathcal{F}(\boldsymbol{f})(u,v)\mathcal{F}(g)(u,v).
\end{aligned}$$

Remark 4.4 *The convolution theorems for quaternion Fourier transform was given in [40]. Lemma 4.1 is following the idea of Theorem 13 and Lemma 14 in [40]. For completeness, we proof the convolution formula in Eq. (4.21).*

Proposition 4.2 *Let $\psi_n(x,y) \in \mathcal{L}^1(\mathbb{R}^2;\mathbb{H})$ be the QPSWFs associated with QLCTs and $\tilde{\psi}_n(x,y) = e^{\mathbf{i}\frac{ca_1}{2b_1}x^2}\psi_n(x,y)e^{\mathbf{j}\frac{ca_2}{2b_2}y^2}$, $\{\tilde{\psi}_n(x,y)\}_{n=0}^{\infty}$ satisfies*

$$\tilde{\psi}_n(u,v) = \int_{\mathbb{R}^2} \tilde{\psi}_n(x,y)\frac{\sin\sigma(x-u)}{\pi(x-u)}\frac{\sin\sigma(y-v)}{\pi(y-v)}dxdy, \tag{4.22}$$

which extends the integral of $\tilde{\psi}_n(x,y)$ from $\boldsymbol{\tau}$ to $\mathbb{R}^2$.

Proof. Let $p_{\boldsymbol{\tau}}(x,y) := \begin{cases} 1, & (x,y) \in \boldsymbol{\tau}, \\ 0, & otherwise, \end{cases}$ Eq. (4.18) is actually a convolution of $p_{\boldsymbol{\tau}}(x,y)\tilde{\psi}_n(x,y)$ with two-dimensional *sinc* kernel $\frac{\sin(\sigma x)}{\pi x}\frac{\sin(\sigma y)}{\pi y}$ as follows

$$\mu_n\tilde{\psi}_n(u,v) = \int_{\mathbb{R}^2} p_{\boldsymbol{\tau}}(x,y)\tilde{\psi}_n(x,y)\frac{\sin\sigma(x-u)}{\pi(x-u)}\frac{\sin\sigma(y-v)}{\pi(y-v)}dxdy. \tag{4.23}$$

Denote $\phi(x,y) := p_{\boldsymbol{\tau}}(x,y)\tilde{\psi}_n(x,y)$. From Lemma 4.1, let $g(x,y) = \frac{\sin\sigma x}{\pi x}\frac{\sin\sigma y}{\pi y}$, the $g(x,y) = g(-x,y)$ and its QFT $p_{\boldsymbol{\sigma}}(u,v)$ is real valued function. Then taking QFT to the both sides of Eq. (4.23), we have

$$\mu_n\mathcal{F}(\tilde{\psi}_n)(u',v') = \mathcal{F}(\phi)(u',v')p_{\boldsymbol{\sigma}}(u',v'). \tag{4.24}$$

Immediately, we obtain that $\mathcal{F}(\tilde{\psi}_n)(u',v') = 0$ for $|u'| > \sigma$ *and* $|v'| > \sigma$, i.e.,

$$\mathcal{F}(\tilde{\psi}_n)(u',v') = \mathcal{F}(\tilde{\psi}_n)(u',v')p_{\boldsymbol{\sigma}}(u',v'). \tag{4.25}$$

Here $p_{\boldsymbol{\sigma}}(x,y) := \begin{cases} 1, & (x,y) \in \boldsymbol{\sigma}, \\ 0, & otherwise. \end{cases}$ From Lemma 4.1, taking the inverse QFT on both sides of the above equation, it follows that $\tilde{\psi}_n$ satisfies Eq. (4.22), which extends the integral domain of $\tilde{\psi}_n(x,y)$ from $\boldsymbol{\tau}$ to $\mathbb{R}^2$. □

The Propositions 4.3 and 4.4 follow from the general theory of integral equations of Hermitian kernel and are stated without proof [10, 11].

Proposition 4.3 (Eigenvalues) *Eq. (4.18) has solutions for real or complex μ_n. These values are a monotonically decreasing sequence, $1 > |\mu_0| > |\mu_1| > ... > |\mu_n| > ...$, and satisfy $\lim_{n\to\infty}|\mu_n| = 0$.*

Proposition 4.4 (Orthogonal in $\boldsymbol{\tau}$) *For different eigenvalues $\{\mu_n\}_{n=0}^{\infty}$, the corresponding eigenfunctions $\{\tilde{\psi}_n(x,y)\}_{n=0}^{\infty}$ are an orthonormal set in $\boldsymbol{\tau}$, i.e.,*

$$\int_{\tau} \tilde{\psi}_n(x,y)\overline{\tilde{\psi}_m(x,y)}dxdy = \begin{cases} \mu_n, & m=n, \\ 0, & otherwise. \end{cases} \tag{4.26}$$

Proposition 4.5 (Orthogonal in $\mathbb{R}^2$) *The eigenfunctions $\{\tilde{\psi}_n(x,y)\}_{n=0}^{\infty}$ form an orthonormal system in $\mathbb{R}^2$, i.e.,*

$$\int_{\mathbb{R}^2} \tilde{\psi}_n(x,y)\overline{\tilde{\psi}_m(x,y)}dxdy = \begin{cases} 1, & m=n, \\ 0, & otherwise. \end{cases} \tag{4.27}$$

Proof. Combining Eq. (4.18), the orthogonality in $\mathbb{R}^2$ can be immediately deduced as follows

$$\begin{aligned}
&\int_{\mathbb{R}^2} \tilde{\psi}_n(x,y)\overline{\tilde{\psi}_m(x,y)}dxdy \\
=\ & \int_{\mathbb{R}^2} \left(\frac{1}{\mu_n}\int_{\tau} \tilde{\psi}_n(s,t)\frac{\sin\sigma(x-s)}{\pi(x-s)}\frac{\sin\sigma(y-t)}{\pi(y-t)}dsdt\right) \\
&\overline{\left(\frac{1}{\mu_m}\int_{\tau} \tilde{\psi}_m(u,v)\frac{\sin\sigma(x-u)}{\pi(x-u)}\frac{\sin\sigma(y-v)}{\pi(y-v)}dudv\right)}dxdy \\
=\ & \frac{1}{\mu_n\mu_m}\int_{\tau}\int_{\tau} \tilde{\psi}_n(s,t)\overline{\tilde{\psi}_m(u,v)}dsdtdudv \\
&\left(\int_{\mathbb{R}^2} \frac{\sin\sigma(x-s)}{\pi(x-s)}\frac{\sin\sigma(y-t)}{\pi(y-t)}\frac{\sin\sigma(x-u)}{\pi(x-u)}\frac{\sin\sigma(y-v)}{\pi(y-v)}dxdy\right) \\
=\ & \frac{1}{\mu_n\mu_m}\int_{\tau}\left(\int_{\tau} \tilde{\psi}_n(s,t)\frac{\sin\sigma(s-u)}{\pi(s-u)}\frac{\sin\sigma(t-v)}{\pi(t-v)}dsdt\right)\overline{\tilde{\psi}_m(u,v)}dudv \\
=\ & \frac{1}{\mu_m}\int_{\tau} \tilde{\psi}_n(u,v)\overline{\tilde{\psi}_m(u,v)}dudv = \begin{cases} 1, & m=n, \\ 0, & otherwise. \end{cases}
\end{aligned}$$

□

5. Main Results

In the present section, we will consider the energy concentration problem of bandlimited $\mathbb{H}$-valued signals in fixed spatial and QLCTs-frequency domains. The definitions and notations of bandlimited $\mathbb{H}$-valued signals associated with QLCTs and QFT are introduced in the following.

Definition 5.1 ($\boldsymbol{\sigma}$-bandlimited $\mathbb{H}$-valued signal associated with QLCTs) *an $\mathbb{H}$-valued signal $\boldsymbol{f}(x,y)$ with finite energy is $\boldsymbol{\sigma}$-bandlimited associated with QLCTs, if its QLCTs vanishes for all (u,v) outside the region $\boldsymbol{\sigma}$, i.e.,*

$$\mathcal{L}(\boldsymbol{f})(u,v) = 0, \quad \text{for } (u,v) \in \mathbb{R}^2 \setminus \boldsymbol{\sigma}. \tag{5.28}$$

Denote $\mathscr{B}_{\boldsymbol{\sigma}}$ the set of $\boldsymbol{\sigma}$-bandlimited $\mathbb{H}$-valued signals associated with QLCTs, i.e.,

$$\mathscr{B}_{\boldsymbol{\sigma}} := \left\{ f \in \mathcal{L}^2(\mathbb{R}^2;\mathbb{H}) \middle| supp(\mathcal{L}(\boldsymbol{f}(u,v))) \in \boldsymbol{\sigma} \right\}. \tag{5.29}$$

Definition 5.2 ($\boldsymbol{\sigma}$-bandlimited $\mathbb{H}$-valued signal associated with QFT) *an $\mathbb{H}$-valued signal $\boldsymbol{f}(x,y)$ with finite energy is $\boldsymbol{\sigma}$-bandlimited associated with QFT, if its QFT vanishes for all (u,v) outside the region $\boldsymbol{\sigma}$, i.e.,*

$$\mathcal{F}(\boldsymbol{f})(u,v) = 0, \quad \text{for } (u,v) \in \mathbb{R}^2 \setminus \boldsymbol{\sigma}. \tag{5.30}$$

Denote $\tilde{\mathscr{B}}_{\boldsymbol{\sigma}}$ the set of the $\boldsymbol{\sigma}$-bandlimited $\mathbb{H}$-valued signals associated with QFT, i.e.,

$$\tilde{\mathscr{B}}_{\boldsymbol{\sigma}} := \left\{ f \in \mathcal{L}^2(\mathbb{R}^2;\mathbb{H}) \middle| supp(\mathcal{F}(\boldsymbol{f}(u,v))) \in \boldsymbol{\sigma} \right\}. \tag{5.31}$$

Note that the relationship between QLCT and QFT for an $\mathbb{H}$-valued signal $\boldsymbol{f}$

$$\mathcal{F}(\tilde{\boldsymbol{f}})\left(\frac{u}{b_1}, \frac{v}{b_2}\right) = 2\pi\sqrt{b_1}\mathbf{i}e^{-\mathbf{i}\frac{d_1}{2b_1}u^2}\mathcal{L}(\boldsymbol{f})(u,v)e^{-\mathbf{j}\frac{d_2}{2b_2}v^2}\sqrt{b_2}\mathbf{j}.$$

That is to say if $\boldsymbol{f} \in \mathscr{B}_{\boldsymbol{\sigma}}$, then for the $\mathcal{F}(\tilde{\boldsymbol{f}})\left(\frac{u}{b_1}, \frac{v}{b_2}\right)$, (u,v) is also in $\boldsymbol{\sigma}$, that means

$$(\frac{u}{b_1}, \frac{v}{b_2}) \in [\frac{-\sigma}{b_1}, \frac{\sigma}{b_1}] \times [\frac{-\sigma}{b_2}, \frac{\sigma}{b_2}] =: \tilde{\boldsymbol{\sigma}}. \tag{5.32}$$

Then $\tilde{\boldsymbol{f}} \in \tilde{\mathscr{B}}_{\tilde{\boldsymbol{\sigma}}}$, because

$$\mathcal{F}(\tilde{\boldsymbol{f}})(u,v) = 0, \quad \text{for } (u,v) \in \mathbb{R}^2 \setminus \tilde{\boldsymbol{\sigma}}. \tag{5.33}$$

Now we pay attention to the energy concentration problem associated with QLCTs. To be specific, the energy concentration problem associated with QLCTs aims to obtain the relationship of the following two energy ratios for any $\mathbb{H}$-valued

signal $\boldsymbol{f}$ with finite energy in a fixed spatial and QLCTs-frequency domains, i.e., $\boldsymbol{\tau}$ and $\boldsymbol{\sigma}$,

$$\alpha_{\boldsymbol{f}} := \frac{\| p_{\boldsymbol{\tau}} \boldsymbol{f} \|^2}{\| \boldsymbol{f} \|^2} \quad \text{and} \quad \beta_{\boldsymbol{f}} := \frac{\| p_{\boldsymbol{\sigma}} \mathcal{L}(\boldsymbol{f}) \|^2}{\| \mathcal{L}(\boldsymbol{f}) \|^2}. \tag{5.34}$$

By the Parseval identity in Eq. (3.16), the two ratios can also be obtained by

$$\alpha_{\boldsymbol{f}} = \frac{\| p_{\boldsymbol{\tau}} \tilde{\boldsymbol{f}} \|^2}{\| \tilde{\boldsymbol{f}} \|^2} \quad \text{and} \quad \beta_{\boldsymbol{f}} = \frac{\| p_{\tilde{\boldsymbol{\sigma}}} \mathcal{F}(\tilde{\boldsymbol{f}}) \|^2}{\| \mathcal{F}(\tilde{\boldsymbol{f}}) \|^2}. \tag{5.35}$$

Note that the value of $\alpha_{\boldsymbol{f}}$ and $\beta_{\boldsymbol{f}}$ are real values in $[0, 1]$.

5.1. Energy Concentration Problem for σ-Bandlimited Signals

In this part, we only consider the energy problem for $\boldsymbol{f} \in \mathscr{B}_{\boldsymbol{\sigma}}$, i.e., $\beta_{\boldsymbol{f}} = 1$ and $\tilde{\boldsymbol{f}} \in \tilde{\mathscr{B}}_{\tilde{\boldsymbol{\sigma}}}$. Concretely speaking, given an unit energy $\tilde{\boldsymbol{f}} \in \tilde{\mathscr{B}}_{\tilde{\boldsymbol{\sigma}}}$, the energy concentration problem is finding the maximum of $\alpha_{\boldsymbol{f}}$, i.e.,

$$\max_{\tilde{\boldsymbol{f}}(x,y) \in \tilde{\mathscr{B}}_{\tilde{\boldsymbol{\sigma}}}} \alpha_{\boldsymbol{f}} = \| p_{\boldsymbol{\tau}} \tilde{\boldsymbol{f}} \|^2 . \tag{5.36}$$

Denote the maximum $\alpha_{\boldsymbol{f}}$ as follows

$$\alpha_{max} := \max_{\tilde{\boldsymbol{f}}(x,y) \in \tilde{\mathscr{B}}_{\tilde{\boldsymbol{\sigma}}}} \alpha_{\boldsymbol{f}}. \tag{5.37}$$

Let $\tilde{\boldsymbol{f}}_{\boldsymbol{\tau}}(x, y) := p_{\boldsymbol{\tau}}(x, y) \tilde{\boldsymbol{f}}(x, y)$, we can also reformulate $\alpha_{\boldsymbol{f}}$ as follows

$$\alpha_{\boldsymbol{f}} = \int_{\mathbb{R}^2} \tilde{\boldsymbol{f}}_{\boldsymbol{\tau}}(x, y) \overline{\tilde{\boldsymbol{f}}(x, y)} dx dy. \tag{5.38}$$

We conclude that the maximum α_{max} can be taken if $\tilde{\boldsymbol{f}}_{\boldsymbol{\tau}}(x, y) = \mu \tilde{\boldsymbol{f}}(x, y)$. To derive this fact, the generally cross-correlation function ρ_{fg} of f and $g \in \mathcal{L}^2(\mathbb{R}^2; \mathbb{C})$ was introduced at first [2],

$$\rho_{fg}(s, t) := \int_{\mathbb{R}^2} \overline{f(x, y)} g(s + x, t + y) dx dy. \tag{5.39}$$

Consider the $(s, t) = (0, 0)$, we have $\rho_{fg}(0, 0) = \int_{\mathbb{R}^2} \overline{f(x, y)} g(x, y) dx dy$. From the complex-valued Schwarz's inequality,

$$\left| \int_{\mathbb{R}^2} \overline{f(x, y)} g(x, y) dx dy \right|^2 \leq \int_{\mathbb{R}^2} |f(x, y)|^2 \, dx dy \int_{\mathbb{R}^2} |g(x, y)|^2 \, dx dy. \tag{5.40}$$

the $|\rho_{fg}(0,0)|^2$ takes the maximum value if $f(x,y) = kg(x,y)$, where k is a constant. Similarly, we can define the cross-correlation function $\rho_{\boldsymbol{fg}}$ of $\mathbb{H}$-valued signals $\boldsymbol{f}$ and $\boldsymbol{g} \in \mathcal{L}^2(\mathbb{R}^2;\mathbb{H})$ as follows

$$\rho_{\boldsymbol{fg}}(s,t) := \int_{\mathbb{R}^2} \overline{\boldsymbol{f}(x,y)}\boldsymbol{g}(s+x,t+y)dxdy. \tag{5.41}$$

Since the quaternionic Schwarz's inequality also holds. Then to get the maximum value of $\rho_{\boldsymbol{fg}}(0,0)$, the relationship between $\boldsymbol{f}$ and $\boldsymbol{g}$ satisfies $\boldsymbol{f}(x,y) = \gamma\boldsymbol{g}(x,y)$, where γ is a constant. Here, we find that

$$\alpha_{\boldsymbol{f}} = \rho_{\tilde{\boldsymbol{f}}_{\boldsymbol{\tau}}\tilde{\boldsymbol{f}}}(0,0). \tag{5.42}$$

To achieve the maximum $\alpha_{\boldsymbol{f}}$, the two functions should be the same except a constant factor. For this reason, there exists a constant μ such that $\tilde{\boldsymbol{f}}_{\boldsymbol{\tau}}(x,y) = \mu\tilde{\boldsymbol{f}}(x,y)$.

Let $\mathcal{F}(\tilde{\boldsymbol{f}}_{\boldsymbol{\tau}})$ and $\mathcal{F}(\tilde{\boldsymbol{f}})$ are the QFT for $\tilde{\boldsymbol{f}}_{\boldsymbol{\tau}}$ and $\tilde{\boldsymbol{f}}$, respectively. Taking QFT to both sides of the equation $\tilde{\boldsymbol{f}}_{\boldsymbol{\tau}}(x,y) = \mu\tilde{\boldsymbol{f}}(x,y)$, we have

$$\mathcal{F}(\tilde{\boldsymbol{f}}_{\boldsymbol{\tau}})(u,v) = \mu\mathcal{F}(\tilde{\boldsymbol{f}})(u,v). \tag{5.43}$$

Since $\tilde{\boldsymbol{f}} \in \tilde{\mathscr{B}}_{\tilde{\boldsymbol{\sigma}}}$, then $\tilde{\boldsymbol{f}}_{\boldsymbol{\tau}}(x,y)$ is also in $\tilde{\mathscr{B}}_{\tilde{\boldsymbol{\sigma}}}$, i.e.,

$$\mathcal{F}(\tilde{\boldsymbol{f}}_{\boldsymbol{\tau}})(u,v)p_{\tilde{\boldsymbol{\sigma}}}(u,v) = \mu\mathcal{F}(\tilde{\boldsymbol{f}})(u,v). \tag{5.44}$$

From Lemma 4.1, taking the inverse QFT to the above equation, we have

$$\int_{\mathbb{R}^2} \tilde{\boldsymbol{f}}_{\boldsymbol{\tau}}(s,t)\frac{\sin\sigma(x-s)}{\pi(x-s)}\frac{\sin\sigma(y-t)}{\pi(y-t)}dsdt = \mu\tilde{\boldsymbol{f}}(x,y). \tag{5.45}$$

Substituting $\tilde{\boldsymbol{f}}_{\boldsymbol{\tau}}(s,t) = p_{\boldsymbol{\tau}}(s,t)\tilde{\boldsymbol{f}}(s,t)$ to the above equation, we have

$$\int_{\boldsymbol{\tau}} \tilde{\boldsymbol{f}}(s,t)\frac{\sin\sigma(x-s)}{\pi(x-s)}\frac{\sin\sigma(y-t)}{\pi(y-t)}dsdt = \mu\tilde{\boldsymbol{f}}(x,y), \tag{5.46}$$

which is the low-pass filter form of QPSWFs.

Now we show that $\boldsymbol{\sigma}$-bandlimited $\mathbb{H}$-valued signals satisfying the low-pass filter form Eq. (5.46) can reach the maximum α_{max}.

Theorem 5.1 *If the eigenvalues of the integral equation*

$$\int_{\boldsymbol{\tau}} \tilde{\boldsymbol{f}}(s,t)\frac{\sin\sigma(x-s)}{\pi(x-s)}\frac{\sin\sigma(y-t)}{\pi(y-t)}dsdt = \mu\tilde{\boldsymbol{f}}(x,y), \tag{5.47}$$

have a maximum μ, then $\alpha_{max} = \mu_{max}$. The eigenfunction corresponding to μ_{max} is the function such that α_{max} are reached.

Proof. For any $\boldsymbol{\sigma}$-bandlimited signal $\tilde{\boldsymbol{f}}$, construct a function $\tilde{\boldsymbol{s}}(x, y)$ as follows

$$\tilde{\boldsymbol{s}}(x, y) := \int_{\boldsymbol{\tau}} \tilde{\boldsymbol{f}}(s, t) \frac{\sin \sigma(x - s)}{\pi(x - s)} \frac{\sin \sigma(y - t)}{\pi(y - t)} ds dt. \tag{5.48}$$

Let the QFT of $\tilde{\boldsymbol{s}}(x, y)$ as $\mathcal{F}(\tilde{\boldsymbol{s}})(u, v)$, it follows that

$$\mathcal{F}(\tilde{\boldsymbol{s}})(u, v) = \mathcal{F}(\tilde{\boldsymbol{f}}_{\boldsymbol{\tau}})(u, v) p_{\tilde{\boldsymbol{\sigma}}}(u, v).$$

It means that $\tilde{\boldsymbol{s}} \in \tilde{\mathscr{B}}_{\tilde{\boldsymbol{\sigma}}}$.

Denote the energy ratio $\alpha_{\boldsymbol{s}}$ for $\tilde{\boldsymbol{s}}(x, y)$ in the fixed spatial domain $\boldsymbol{\tau}$ as follows

$$\alpha_{\boldsymbol{s}} = \frac{1}{E_{\boldsymbol{s}}} \int_{\mathbb{R}^2} p_{\boldsymbol{\tau}}(x, y) \tilde{\boldsymbol{s}}(x, y) \overline{\tilde{\boldsymbol{s}}(x, y)} dx dy. \tag{5.49}$$

We conclude that for any $\tilde{\boldsymbol{f}} \in \tilde{\mathscr{B}}_{\tilde{\boldsymbol{\sigma}}}$, $\alpha_{\boldsymbol{f}}$ cannot exceed the $\alpha_{\boldsymbol{s}}$. Direct computations show that the energy of the signal $\tilde{\boldsymbol{s}}(x, y)$ is given as follows

$$\begin{aligned}
E_{\boldsymbol{s}} &= \int_{\mathbb{R}^2} \tilde{\boldsymbol{s}}(x, y) \overline{\tilde{\boldsymbol{s}}(x, y)} dx dy \\
&= \int_{\mathbb{R}^2} \mathcal{F}(\tilde{\boldsymbol{s}})(u, v) \overline{\mathcal{F}(\tilde{\boldsymbol{s}})(u, v)} du dv \\
&= \mathbf{Sc}\left[\int_{\tilde{\boldsymbol{\sigma}}} \mathcal{F}(\tilde{\boldsymbol{f}}_{\boldsymbol{\tau}})(u, v) \overline{\mathcal{F}(\tilde{\boldsymbol{s}})(u, v)} du dv \right] \\
&= \mathbf{Sc}\left[\int_{\mathbb{R}^2} \tilde{\boldsymbol{f}}_{\boldsymbol{\tau}}(x, y) \tilde{\boldsymbol{s}}(x, y) dx dy \right] \\
&= \mathbf{Sc}\left[\int_{\mathbb{R}^2} p_{\boldsymbol{\tau}}(x, y) \tilde{\boldsymbol{f}}(x, y) \overline{\tilde{\boldsymbol{s}}(x, y)} dx dy \right].
\end{aligned}$$

On the other hand, we consider that

$$\begin{aligned}
\alpha_{\boldsymbol{f}} E_{\boldsymbol{f}} &= \int_{\mathbb{R}^2} \tilde{\boldsymbol{f}}_{\boldsymbol{\tau}}(x, y) \overline{\tilde{\boldsymbol{f}}(x, y)} dx dy \\
&= \mathbf{Sc}\left[\int_{\mathbb{R}^2} \mathcal{F}(\tilde{\boldsymbol{f}}_{\boldsymbol{\tau}})(u, v) \overline{\mathcal{F}(\tilde{\boldsymbol{f}})(u, v)} du dv \right] \\
&= \mathbf{Sc}\left[\int_{\tilde{\boldsymbol{\sigma}}} \mathcal{F}(\tilde{\boldsymbol{s}})(u, v) \overline{\mathcal{F}(\tilde{\boldsymbol{f}})(u, v)} du dv \right].
\end{aligned}$$

Since

$$\left| \int_{\tilde{\boldsymbol{\sigma}}} \mathcal{F}(\tilde{\boldsymbol{s}})(u, v) \overline{\mathcal{F}(\tilde{\boldsymbol{f}})(u, v)} du dv \right|^2 \leq \| p_{\tilde{\boldsymbol{\sigma}}} \mathcal{F}(\tilde{\boldsymbol{s}}) \|^2 \| p_{\tilde{\boldsymbol{\sigma}}} \mathcal{F}(\tilde{\boldsymbol{f}}) \|^2, \tag{5.50}$$

and

$$\left|\mathbf{Sc}\left[\int_{\tilde{\sigma}} \mathcal{F}(\tilde{s})(u,v)\overline{\mathcal{F}(\tilde{f})(u,v)}dudv\right]\right|^2 \leq \left|\int_{\tilde{\sigma}} \mathcal{F}(\tilde{s})(u,v)\overline{\mathcal{F}(\tilde{f})(u,v)}dudv\right|^2,$$

simplifying the above three inequalities, we obtain that

$$(\alpha_f E_f)^2 \leq E_s E_f,$$

from which it follows that

$$\alpha_f^2 E_f \leq E_s.$$

We also have the following result for E_s

$$\begin{aligned} E_s^2 &= \left|\mathbf{Sc}\left[\int_{\mathbb{R}^2} p_\tau(x,y)\tilde{\boldsymbol{f}}(x,y)\overline{\tilde{s}(x,y)}dxdy\right]\right|^2 \\ &\leq \left|\int_{\mathbb{R}^2} p_\tau(x,y)\tilde{\boldsymbol{f}}(x,y)\overline{\tilde{s}(x,y)}dxdy\right|^2 \\ &\leq \int_{\mathbb{R}^2} p_\tau(x,y)\tilde{\boldsymbol{f}}(x,y)\overline{\tilde{\boldsymbol{f}}(x,y)}dxdy \int_{\mathbb{R}^2} p_\tau(x,y)\tilde{s}(x,y)\overline{\tilde{s}(x,y)}dxdy. \end{aligned} \tag{5.51}$$

Here, we take $p_\tau(x,y)$ into two parts, i.e., $\left(\sqrt{p_\tau(x,y)}\right)^2$, and use the Schwarz inequality for the above inequality. Clearly, $(E_s)^2 \leq (\alpha_f E_f)(\alpha_s E_s)$, then

$$E_s \leq \alpha_f \alpha_s E_f.$$

Summarizing, we have

$$\alpha_f^2 E_f \leq E_s \leq \alpha_f \alpha_s E_f.$$

That means, for any $\tilde{\boldsymbol{f}} \in \tilde{\mathscr{B}}_{\tilde{\sigma}}$, $\alpha_f \leq \alpha_s$.

If $\alpha_f = \alpha_s$, then Eq. (5.50) and Eq. (5.51) must be equalities. This is attained only by setting $\tilde{s}(x,y) = \alpha_f \tilde{\boldsymbol{f}}(x,y)$ with $E_s = \alpha_f^2 E_f$. It means that $\tilde{\boldsymbol{f}}$ is an eigenfunction of Eq. (5.47) and α_f is the corresponding eigenvalue, i.e., $\mu = \alpha_f$.

At last, we will show that $\alpha_{max} = \mu_{max}$, and the eigenfunction corresponding to μ_{max} is the function such that α_{max} is reached. By definition of $0 \leq \alpha_f \leq 1$, there exists a maximum α_f and we denote the maximum α_f as α_{max} and the corresponding signal as $\tilde{\boldsymbol{f}}_0(x,y)$. As we have shown, the α_{max} corresponding the

eigenfunction satisfies $\tilde{\boldsymbol{s}}(x,y) = \alpha_{\boldsymbol{f}}\tilde{\boldsymbol{f}}(x,y)$. Here, $\tilde{\boldsymbol{s}}(x,y) = \alpha_{\boldsymbol{f}}\tilde{\boldsymbol{f}}(x,y) = \alpha_{\boldsymbol{f}}\tilde{\boldsymbol{f}}_0(x,y)$ corresponds to the maximum eigenvalue of μ_{max}. Hence, $\mu_{max} \leq \alpha_{max}$.

In order to prove that $\mu_{max} = \alpha_{max}$, it suffices to show that $\tilde{\boldsymbol{f}}_0(x,y)$ is an eigenfunction of the integral equation Eq. (5.47), or equivalently, that with $\tilde{\boldsymbol{S}}_0(x,y)$ defined as $\tilde{\boldsymbol{s}}(x,y)$ in Eq. (5.48) with $\alpha_{\boldsymbol{S}_0} = \alpha_{max}$. Obviously, $\alpha_{\boldsymbol{S}} \geq \alpha_{max}$ and $\alpha_{\boldsymbol{S}_0} \leq \alpha_{max}$, because α_{max} is maximum by assumption. The proof is complete. □

Theorem 5.1 shows that for arbitrary unit energy $\boldsymbol{\sigma}$-bandlimited $\mathbb{H}$-valued signal associated with QLCTs the maximum value of $\alpha_{\boldsymbol{f}}$ can be achieved by the QPSWFs. In fact, from the symmetry theorem of Fourier theory [2], there is also a similar integral equation for time-limited signals, which have the maximum $\beta_{\tilde{\boldsymbol{f}}}$. The prove of this conclusion is similar to Theorem 5.1.

Corollary 5.1 *If the eigenvalues of the integral equation*

$$\int_{\tilde{\boldsymbol{\sigma}}} \mathcal{F}(\tilde{\boldsymbol{f}})(u,v)\frac{\sin\tau(x-u)}{\pi(x-u)}\frac{\sin\tau(y-v)}{\pi(y-v)}dudv = \mu\mathcal{F}(\tilde{\boldsymbol{f}})(x,y). \tag{5.52}$$

have a maximum μ, then $\beta_{\tilde{\boldsymbol{f}}}$ have a maximum number β_{max} and $\beta_{max} = \mu_{max}$. The eigenfunction corresponding to μ_{max} is the function such that β_{max} are reached.

The Eq. (5.52) is equivalent to Eq. (5.47) with $u = \frac{\sigma s}{\tau}$ and $v = \frac{\sigma t}{\tau}$.

5.2. Extremal Properties

In this section, we will discuss the relationship of $(\alpha_{\boldsymbol{f}}, \beta_{\boldsymbol{f}})$ in Eq. (5.34) from three cases:

(1) $\boldsymbol{f}(x,y)$ is a $\boldsymbol{\sigma}$-bandlimited signal associated with QLCTs.

(2) $\boldsymbol{f}(x,y)$ is a $\boldsymbol{\tau}$-time-limited signal.

(3) $\boldsymbol{f}(x,y)$ is an arbitrary signal.

The first case follows form the general theory of the $\boldsymbol{f} \in \mathscr{B}_{\boldsymbol{\sigma}}$ in Section 5.1. As we have known $\tilde{\boldsymbol{f}}$ is in $\tilde{\mathscr{B}}_{\tilde{\boldsymbol{\sigma}}}$ when $\boldsymbol{f} \in \mathscr{B}_{\boldsymbol{\sigma}}$, i.e., $\beta_{\boldsymbol{f}} = 1$. From Theorem 5.1, we know that the maximum $\alpha_{\boldsymbol{f}}$ equals the maximum eigenvalue μ_0 in Eq. (5.47). Using the expansion for the $\tilde{\boldsymbol{f}} \in \tilde{\mathscr{B}}_{\tilde{\boldsymbol{\sigma}}}$, $\tilde{\boldsymbol{f}}(x,y) = \Sigma_{n=0}^{\infty} a_n\tilde{\psi}_n(x,y)$, where $a_n := \int_{\mathbb{R}^2} \tilde{\boldsymbol{f}}(x,y)\overline{\psi_n(x,y)}dxdy$. It is clear that $\alpha_{\boldsymbol{f}} = \int_{\boldsymbol{\tau}} \tilde{\boldsymbol{f}}(x,y)\overline{\tilde{\boldsymbol{f}}(x,y)}dxdy = \Sigma_{n=0}^{\infty}\mu_n a_n^2 \leq \mu_0\Sigma_{n=0}^{\infty}a_n^2 = \mu_0$. Hence, $\alpha_{\boldsymbol{f}} \leq \mu_0$. If $\alpha_{\boldsymbol{f}} = \mu_0$, then $\tilde{\boldsymbol{f}}(x,y) = \tilde{\psi}_0(x,y)$. If $\alpha_{\boldsymbol{f}} < \mu_0$,

then we can find a signal $\boldsymbol{f} \in \mathscr{B}_{\boldsymbol{\sigma}}$ whose energy ratio in spatial domain equals $\alpha_{\boldsymbol{f}}$, and in this case, $\tilde{\boldsymbol{f}}(x, y)$ is not unique.

The second case means $\alpha_{\boldsymbol{f}} = 1$. From the property of symmetry of the QLCT we conclude that all the properties for signals $\boldsymbol{f} \in \mathscr{B}_{\boldsymbol{\sigma}}$ have corresponding time-limited counterparts. Reversing (x, y) and (u, v), we conclude that $\beta_{\boldsymbol{f}} \leq \mu_0$. Specially, if $\beta_{\boldsymbol{f}} = \mu_0$, then $\tilde{\boldsymbol{f}}(x, y) = \frac{p_{\boldsymbol{\tau}}(x,y)\tilde{\psi}_0(x,y)}{\sqrt{\mu_0}}$.

For the third case, considering arbitrary signals with $\alpha_{\boldsymbol{f}} < 1$, we aim to find the maximum $\beta_{\boldsymbol{f}}$ and the corresponding signal $\boldsymbol{f}(x, y)$. If $\alpha_{\boldsymbol{f}} \leq \mu_0$, as we noted in the case of $\boldsymbol{f} \in \mathscr{B}_{\boldsymbol{\sigma}}$, we can find $\tilde{\boldsymbol{f}} \in \tilde{\mathscr{B}}_{\tilde{\boldsymbol{\sigma}}}$ with energy ration $\alpha_{\boldsymbol{f}}$, hence, $\beta_{max} = 1$. Therefore, we only need to consider the case of $\alpha_{\boldsymbol{f}} > \mu_0$.

Theorem 5.2 *The maximum β_{max} of $\beta_{\boldsymbol{f}}$ must satisfy the following equation*

$$\arccos \sqrt{\beta_{\boldsymbol{f}}} + \arccos \sqrt{\alpha_{\boldsymbol{f}}} = \arccos \sqrt{\mu_0}, \tag{5.53}$$

where μ_0 is the largest eigenvalues of Eq. (4.18) and the corresponding $\tilde{\boldsymbol{f}}$ for the maximum β_{max} is given by

$$\tilde{\boldsymbol{f}}(x, y) = \sqrt{\frac{1-\alpha_{\boldsymbol{f}}}{1-\mu_0}} p_{\boldsymbol{\tau}}(x, y)\tilde{\psi}_0(x, y) + \left(\sqrt{\frac{\alpha_{\boldsymbol{f}}}{\mu_0}} - \alpha_{\boldsymbol{f}} \right) \tilde{\psi}_0(x, y). \tag{5.54}$$

Proof. Before giving the proof to Eq. (5.53), we first need to present the following fact. Given a function $\tilde{\boldsymbol{f}}$ with spatial projection $p_{\boldsymbol{\tau}}\tilde{\boldsymbol{f}}$ and frequency projection $p_{\tilde{\boldsymbol{\sigma}}}\mathcal{F}(\tilde{\boldsymbol{f}})$, we construct a new function as follows

$$\tilde{\boldsymbol{f}}_1(x, y) := a p_{\boldsymbol{\tau}}\tilde{\boldsymbol{f}}(x, y) + b\mathcal{F}^{-1}\Big(p_{\tilde{\boldsymbol{\sigma}}}\mathcal{F}(\tilde{\boldsymbol{f}})\Big)(x, y), \tag{5.55}$$

where a and b are two constants such that the energy of $\boldsymbol{g}(x, y)$ is minimum, where

$$\boldsymbol{g}(x, y) := \tilde{\boldsymbol{f}}(x, y) - \tilde{\boldsymbol{f}}_1(x, y). \tag{5.56}$$

Denote $\alpha_{\boldsymbol{f}}, \beta_{\boldsymbol{f}}$ and $\alpha_{\boldsymbol{f}_1}, \beta_{\boldsymbol{f}_1}$ the energy ratios for $\tilde{\boldsymbol{f}}(x, y)$ and $\tilde{\boldsymbol{f}}_1(x, y)$ as Eq. (5.34), respectively. We conclude that $\alpha_{\boldsymbol{f}_1} \geq \alpha_{\boldsymbol{f}}, \beta_{\boldsymbol{f}_1} \geq \beta_{\boldsymbol{f}}$.

Suppose the energy of $\tilde{\boldsymbol{f}}(x, y)$ equals to 1 and we rewrite $\alpha_{\boldsymbol{f}}$, $\beta_{\boldsymbol{f}}$ as follows

$$\begin{aligned} \alpha_{\boldsymbol{f}} &= \left\langle p_{\boldsymbol{\tau}}\tilde{\boldsymbol{f}}, p_{\boldsymbol{\tau}}\tilde{\boldsymbol{f}} \right\rangle, \\ \beta_{\boldsymbol{f}} &= \left\langle p_{\tilde{\boldsymbol{\sigma}}}\mathcal{F}(\tilde{\boldsymbol{f}}), p_{\tilde{\boldsymbol{\sigma}}}\mathcal{F}(\tilde{\boldsymbol{f}}) \right\rangle. \end{aligned} \tag{5.57}$$

From the orthogonality principle [2], it follows that

$$\left\langle p_{\boldsymbol{\tau}}\tilde{\boldsymbol{f}}, \boldsymbol{g} \right\rangle = 0, \quad \text{and} \quad \left\langle \mathcal{F}^{-1}\Big(p_{\tilde{\boldsymbol{\sigma}}}\mathcal{F}(\tilde{\boldsymbol{f}})\Big), \boldsymbol{g} \right\rangle = 0, \tag{5.58}$$

which means $\left\langle \tilde{\boldsymbol{f}}_1, \boldsymbol{g} \right\rangle = 0$. Meanwhile, we have $E_{\boldsymbol{f}_1}$ of $\tilde{\boldsymbol{f}}_1$ by

$$E_{\boldsymbol{f}_1} := \left\langle \tilde{\boldsymbol{f}}_1, \tilde{\boldsymbol{f}}_1 \right\rangle = 1 - E_{\boldsymbol{g}}. \tag{5.59}$$

Now we denote two energy for the projection of $\boldsymbol{g}(x, y)$ as follows

$$E_{p_\tau \boldsymbol{g}} := \left\langle p_\tau \boldsymbol{g}, p_\tau \boldsymbol{g} \right\rangle, \quad \text{and} \quad E_{p_{\tilde{\sigma}} \mathcal{F}(\boldsymbol{g})} := \left\langle p_{\tilde{\sigma}} \mathcal{F}(\boldsymbol{g}), p_{\tilde{\sigma}} \mathcal{F}(\boldsymbol{g}) \right\rangle. \tag{5.60}$$

The $E_{p_\tau f}$ and $E_{p_{\tilde{\sigma}} \mathcal{F}(\boldsymbol{f})}$ will be simply written as E_τ and $E_{\tilde{\sigma}}$ in the following, respectively. Since $\tilde{\boldsymbol{f}}_1(x, y) = \tilde{\boldsymbol{f}}(x, y) - \boldsymbol{g}(x, y)$, we have

$$\begin{aligned} &\left\langle p_\tau \tilde{\boldsymbol{f}}_1, p_\tau \tilde{\boldsymbol{f}}_1 \right\rangle = \alpha_{\boldsymbol{f}_1} E_{\boldsymbol{f}_1} = \alpha_{\boldsymbol{f}} + E_\tau, \\ &\left\langle p_{\tilde{\sigma}} \mathcal{F}(\tilde{\boldsymbol{f}}_1), p_{\tilde{\sigma}} \mathcal{F}(\tilde{\boldsymbol{f}}_1) \right\rangle = \beta_{\boldsymbol{f}_1} E_{\boldsymbol{f}_1} = \beta_{\boldsymbol{f}} + E_{\tilde{\sigma}}. \end{aligned} \tag{5.61}$$

Therefore, $\alpha_{\boldsymbol{f}_1} \geq \alpha_{\boldsymbol{f}}$ and $\beta_{\boldsymbol{f}_1} \geq \beta_{\boldsymbol{f}}$. That means, in order to get the maximum $\beta_{\boldsymbol{f}}$, we can formula a function as follows

$$\tilde{\boldsymbol{f}} = a p_\tau \tilde{\boldsymbol{f}} + b \mathcal{F}^{-1}\left(p_{\tilde{\sigma}} \mathcal{F}(\tilde{\boldsymbol{f}}) \right). \tag{5.62}$$

Taking QFT to both sides for Eq. (5.62) and then taking frequency projection, we have

$$\mathcal{F}\left(\tilde{\boldsymbol{f}}\right) p_{\tilde{\sigma}} = a p_{\tilde{\sigma}} \mathcal{F}\left(\tilde{\boldsymbol{f}}\right) * \left(\frac{\sin(\tau u)}{\pi u} \frac{\sin(\tau v)}{\pi v} \right) + b p_{\tilde{\sigma}} \mathcal{F}(\tilde{\boldsymbol{f}}). \tag{5.63}$$

Rearranging this formula, we obtain that

$$(1 - b) \mathcal{F}\left(\tilde{\boldsymbol{f}}\right) p_{\tilde{\sigma}} = a p_{\tilde{\sigma}} \left[\mathcal{F}\left(\tilde{\boldsymbol{f}}\right) * \left(\frac{\sin(\tau u)}{\pi u} \frac{\sin(\tau v)}{\pi v} \right) \right]. \tag{5.64}$$

Taking inverse QFT to the above equation, we have

$$\begin{aligned} &\frac{1 - b}{a} \mathcal{F}^{-1}\left(\mathcal{F}\left(\tilde{\boldsymbol{f}}\right) p_{\tilde{\sigma}} \right) \\ = \;& \mathcal{F}^{-1}\left(\mathcal{F}\left(\tilde{\boldsymbol{f}}\right) * \left(\frac{\sin(\tau u)}{\pi u} \frac{\sin(\tau v)}{\pi v} \right) \right) * \left(\frac{\sin(\sigma x)}{\pi x} \frac{\sin(\sigma y)}{\pi y} \right). \end{aligned} \tag{5.65}$$

On the other hand, taking the spatial projection to Eq. (5.62), we get

$$p_\tau(x, y) \tilde{\boldsymbol{f}}(x, y) = a p_\tau(x, y) \tilde{\boldsymbol{f}}(x, y) + b \mathcal{F}^{-1}\left(p_{\tilde{\sigma}} \mathcal{F}(\tilde{\boldsymbol{f}}) \right)(x, y) p_\tau(x, y). \tag{5.66}$$

Rearranging this equation, it becomes

$$(1-a)p_{\tau}(x,y)\tilde{\boldsymbol{f}}(x,y) = bp_{\tau}(x,y)\mathcal{F}^{-1}\left(p_{\tilde{\sigma}}\mathcal{F}(\tilde{\boldsymbol{f}})\right)(x,y). \tag{5.67}$$

Taking QFT on both sides to the above equation, it follows that

$$(1-a)\mathcal{F}\left(\tilde{\boldsymbol{f}}\right) * \left(\frac{\sin(\tau u)}{\pi u}\frac{\sin(\tau v)}{\pi v}\right) = b\left(p_{\tilde{\sigma}}\mathcal{F}(\tilde{\boldsymbol{f}})\right) * \left(\frac{\sin(\tau u)}{\pi u}\frac{\sin(\tau v)}{\pi v}\right). \tag{5.68}$$

Applying Eq. (5.65) and Eq. (5.68), we have

$$\begin{aligned}
&\frac{1-b}{a}\mathcal{F}^{-1}\left(\mathcal{F}\left(\tilde{\boldsymbol{f}}\right)p_{\tilde{\sigma}}\right)\\
=\;& \mathcal{F}^{-1}\left(\mathcal{F}\left(\tilde{\boldsymbol{f}}\right) * \left(\frac{\sin(\tau u)}{\pi u}\frac{\sin(\tau v)}{\pi v}\right)\right) * \left(\frac{\sin(\sigma x)}{\pi x}\frac{\sin(\sigma y)}{\pi y}\right)\\
=\;& \frac{b}{1-a}\mathcal{F}^{-1}\left(\left(p_{\tilde{\sigma}}\mathcal{F}(\tilde{\boldsymbol{f}})\right) * \left(\frac{\sin(\tau u)}{\pi u}\frac{\sin(\tau v)}{\pi v}\right)\right) * \left(\frac{\sin(\sigma x)}{\pi x}\frac{\sin(\sigma y)}{\pi y}\right)\\
=\;& \frac{b}{1-a}\mathcal{F}^{-1}\left(p_{\tilde{\sigma}}\mathcal{F}(\tilde{\boldsymbol{f}})\right)p_{\tau}(x,y) * \left(\frac{\sin(\sigma x)}{\pi x}\frac{\sin(\sigma y)}{\pi y}\right).
\end{aligned}$$

Simplifying the above equality, we obtain that

$$\frac{(1-a)(1-b)}{ab}\mathcal{F}^{-1}\left(\mathcal{F}\left(\tilde{\boldsymbol{f}}\right)p_{\tilde{\sigma}}\right) = p_{\tau}(x,y)\mathcal{F}^{-1}\left(\mathcal{F}\left(\tilde{\boldsymbol{f}}\right)p_{\tilde{\sigma}}\right) * \left(\frac{\sin\sigma x}{\pi x}\frac{\sin\sigma y}{\pi y}\right).$$

From above equality, we find that $\mathcal{F}^{-1}\left(\mathcal{F}\left(\tilde{\boldsymbol{f}}\right)p_{\tilde{\sigma}}\right)$ is one of QPSWFs for Eq. (4.18) and the corresponding eigenvalue is $\frac{(1-a)(1-b)}{ab}$. By the relationship between $\tilde{\boldsymbol{f}}$ and $\mathcal{F}^{-1}\left(\mathcal{F}\left(\tilde{\boldsymbol{f}}\right)p_{\tilde{\sigma}}\right)$ in Eq. (5.67), we conclude that $\tilde{\boldsymbol{f}}$ in Eq. (5.62) can be rewritten as

$$\tilde{\boldsymbol{f}}(x,y) = A\tilde{\psi}(x,y) + Bp_{\tau}(x,y)\tilde{\psi}(x,y). \tag{5.69}$$

Now, we compute the inner product of the above equation with $\tilde{\boldsymbol{f}}$ and $p_{\tau}\tilde{\boldsymbol{f}}$ respectively. Since $E_{\boldsymbol{f}} = 1$ for $\tilde{\boldsymbol{f}}$, we have

$$\begin{aligned}
1 &= A^2 + \mu B^2 + 2AB\mu, \\
\alpha_{\boldsymbol{f}} &= (A+B)^2\mu.
\end{aligned} \tag{5.70}$$

Then we have $A = \sqrt{\frac{1-\alpha_{\boldsymbol{f}}}{1-\mu}}$ and $B = \sqrt{\frac{\alpha_{\boldsymbol{f}}}{\mu}} - \sqrt{\frac{1-\alpha_{\boldsymbol{f}}}{1-\mu}}$. It follows that

$$\beta_{\boldsymbol{f}} = \langle p_{\tilde{\sigma}}\mathcal{F}(\tilde{\psi}), p_{\tilde{\sigma}}\mathcal{F}(\tilde{\psi})\rangle = (A+B\mu)^2. \tag{5.71}$$

With $\sqrt{\alpha_f} = \cos\theta$ and $\sqrt{\mu} = \cos\theta_1$, the parameters become $A = \frac{\sin\theta_1}{\sin\theta}$ and $B = \frac{\cos\theta_1}{\cos\theta} - \frac{\sin\theta_1}{\sin\theta}$. That means

$$\sqrt{\beta_f} = \frac{\sin\theta}{\sin\theta_1} + \Big(\frac{\cos\theta}{\cos\theta_1} - \frac{\sin\theta}{\sin\theta_1}\Big)\cos^2\theta_1 = \cos(\theta - \theta_1), \tag{5.72}$$

from which it follows that

$$\arccos\sqrt{\beta_f} + \arccos\sqrt{\alpha_f} = \arccos\sqrt{\mu}. \tag{5.73}$$

In order to get the maximal β_f, we must take the largest $\mu = \mu_0$. The corresponding function is

$$\tilde{\boldsymbol{f}}(x,y) = \sqrt{\frac{1-\alpha_f}{1-\mu_0}}\tilde{\psi}_0(x,y) + (\sqrt{\frac{\alpha_f}{\mu_0}} - \sqrt{\frac{1-\alpha_f}{1-\mu_0}})p_\tau\tilde{\psi}_0(x,y). \tag{5.74}$$

The proof is complete. □

Until now we have discussed all the relationships of (α_f, β_f), as well as the signals to reach the maximum value of β_f for different conditions of α_f.

Example 5.1 *Now we give some comparison examples to intuitively illustrate the concentration levels of QPSWFs associated with QLCTs. The widely used Gaussian function will be compared with QPSWFs. In Theorem 5.1, we have shown that QPSWFs are the most energy concentred $\boldsymbol{\sigma}$-bandlimited signals.*

Now, a $\boldsymbol{\sigma}$-bandlimited Gaussian function is constructed at first. Consider the truncated Gaussian function $\boldsymbol{g}(x,y)$ in QLCTs-frequency domain as follows

$$G(u,v) = \frac{p_{\boldsymbol{\sigma}}(u,v)e^{-(u^2+v^2)}}{\| p_{\boldsymbol{\sigma}}e^{-(u^2+v^2)} \|}, \tag{5.75}$$

where $G(u,v)$ is the QLCT of $\boldsymbol{g}(x,y)$. Obviously, $G(u,v)$ has unit energy. This $\boldsymbol{\sigma}$-bandlimited Gaussian function $\boldsymbol{g}(x,y)$ in spatial domain becomes

$$\boldsymbol{g}(x,y) = \frac{1}{\| p_{\boldsymbol{\sigma}}e^{-(u^2+v^2)} \|}\mathcal{L}^{-1}\Big(p_{\boldsymbol{\sigma}}(u,v)e^{-(u^2+v^2)}\Big). \tag{5.76}$$

As for the QPSWFs, by means of the classical one-dimensional PSWFs of zero order we now construct a special QPSWF as follows

$$\psi_0(x,y) = \frac{\varphi_0(x)\varphi_0(y)}{\| \varphi_0(x)\varphi_0(y) \|}, \tag{5.77}$$

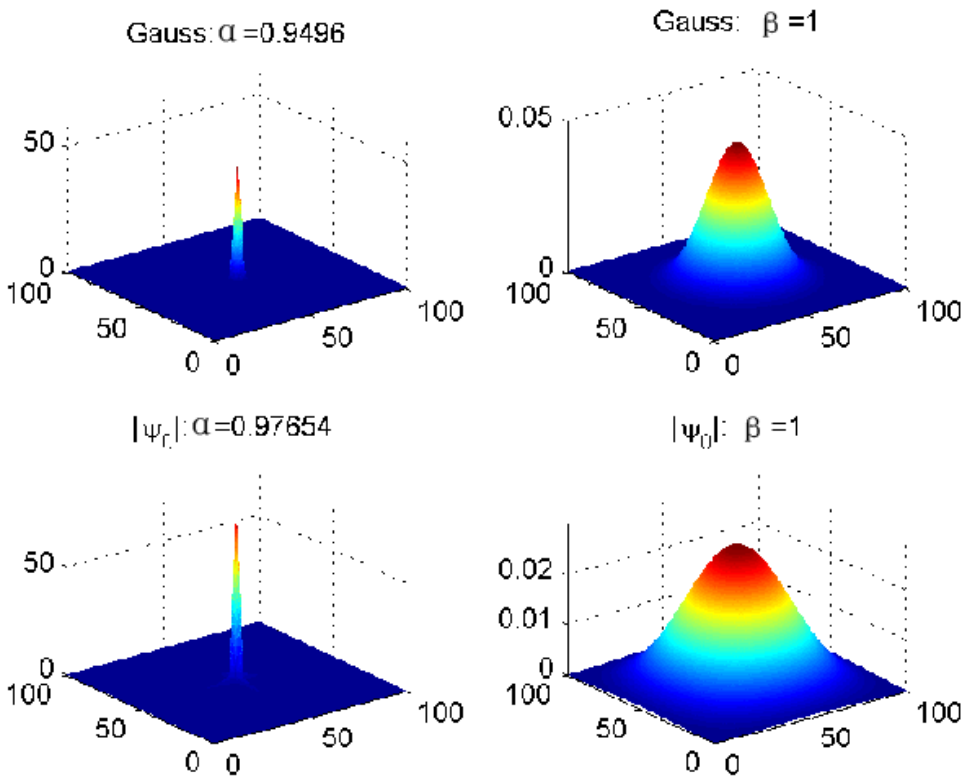

Figure 1: $\boldsymbol{\sigma}$-bandlimited $\boldsymbol{g}(x,y)$ associated with QFT and the modulus of $\psi_0(x,y)$ in time and QFT-frequency domains.

where φ_0 is the first one-dimensional zero order PSWF. Here, we construct the QPSWF under the condition of $c = 1$. The QLCTs for the QPSWF becomes

$$\mathcal{L}(\psi_0)(u,v) = \frac{1}{\| \varphi_0(x)\varphi_0(y) \|}\mathcal{L}(\varphi_0(x)\varphi_0(y)). \tag{5.78}$$

For both of the $\boldsymbol{\sigma}$-bandlimited signals above, the energy ratios β equal to 1 in QLCT-frequency domain. The energy ratio pair in spatial and frequency in the comparison is noted as $(\alpha,\beta) := (\alpha_{\boldsymbol{f}},\beta_{\boldsymbol{f}})$.

In Fig. 1 and Fig. 2, we will show two pairs of the energy ratios α for $\boldsymbol{g}(x,y)$ and $\psi_0(x,y)$ in spatial domain associated with QLCT with two kinds of different parameter matrices. In Fig. 1 we set the parameter matrices of QLCT A_i =

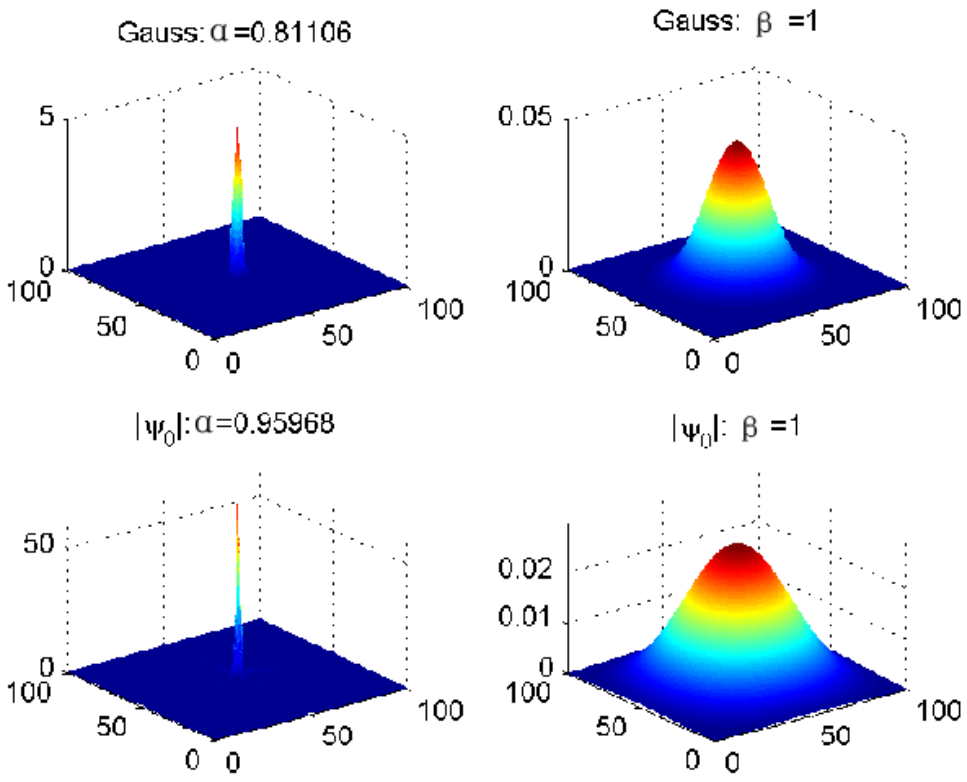

Figure 2: $\boldsymbol{\sigma}$-bandlimited $\boldsymbol{g}(x,y)$ associated with QLCTs and the modulus of $\psi_0(x,y)$ in time and QLCT-frequency domains with $a_1 = a_2 = 0$, $b_1 = b_2 = 1$, $c_1 = c_2 = -1$, $d_1 = d_2 = 0.1$.

$\begin{pmatrix} 0 & 1 \\ -1 & 0 \end{pmatrix}$, $i = 1, 2$, *which is already a QFT. In this case, the energy ratios* α *for* $\boldsymbol{g}(x,y)$ *and* $\psi_0(x,y)$ *are very close. However, in Fig. 2 we set the parameter matrices of QLCT* $A_i = \begin{pmatrix} 0.3 & 1 \\ -1 & 0 \end{pmatrix}$, $i = 1, 2$. *In this case, the energy ratio* α *for* $\boldsymbol{g}(x,y)$ *is* 0.81106 *and* α *for* $\psi_0(x,y)$ *is* 0.95968. *In fact, we just change the parameters* a_i, $i = 1, 2$ *from* 0 *to* 0.3. *That means, for QPSWFs the energy is more concentred then truncated Gaussian function.*

As for the $\boldsymbol{\tau}$ *time-limited function, there are the similar results like* $\boldsymbol{\sigma}$*-bandlimited cases. We also list two pairs of the energy ratios* β *for* $\boldsymbol{g}(x,y)$ *and* $\psi_0(x,y)$ *in QLCT-frequency domains in Fig. 3 and Fig. 4. In Fig. 3 we also set the parame-*

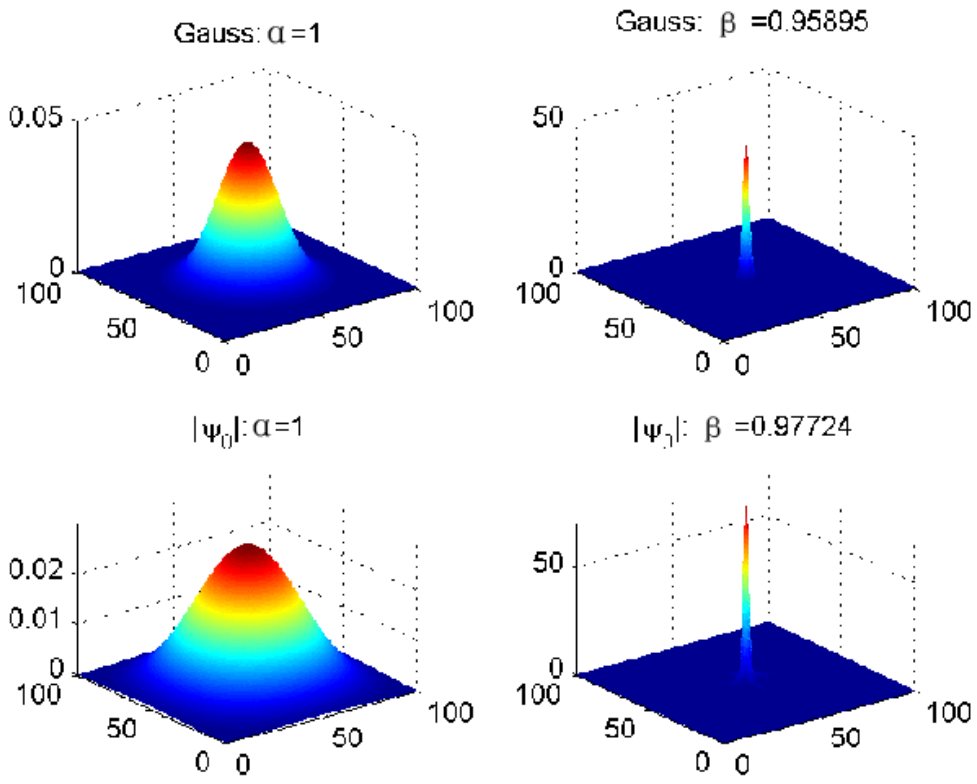

Figure 3: τ-time-limited $\boldsymbol{g}(x,y)$ associated with QFT and the modulus of $\psi_0(x,y)$ in time and QFT-frequency domains.

ter matrices of QLCT to be the QFT. The parameter matrices of QLCT in Fig. 4 is the same as that in Fig. 2. In this two pair cases, you may see the energy ratios β for $\boldsymbol{g}(x,y)$ and $\psi_0(x,y)$ are very close. But one more thing different from Fig. 1 and Fig. 2 is that the energy ratios β for $\boldsymbol{g}(x,y)$ and $\psi_0(x,y)$ associated with QFT is smaller than the energy ratios β for $\boldsymbol{g}(x,y)$ and $\psi_0(x,y)$ associated with the second parameter matrices. That means, the parameter matrices of QLCT is vary important. In some sense, for specific conditions the results for QLCT will be better than QFT.

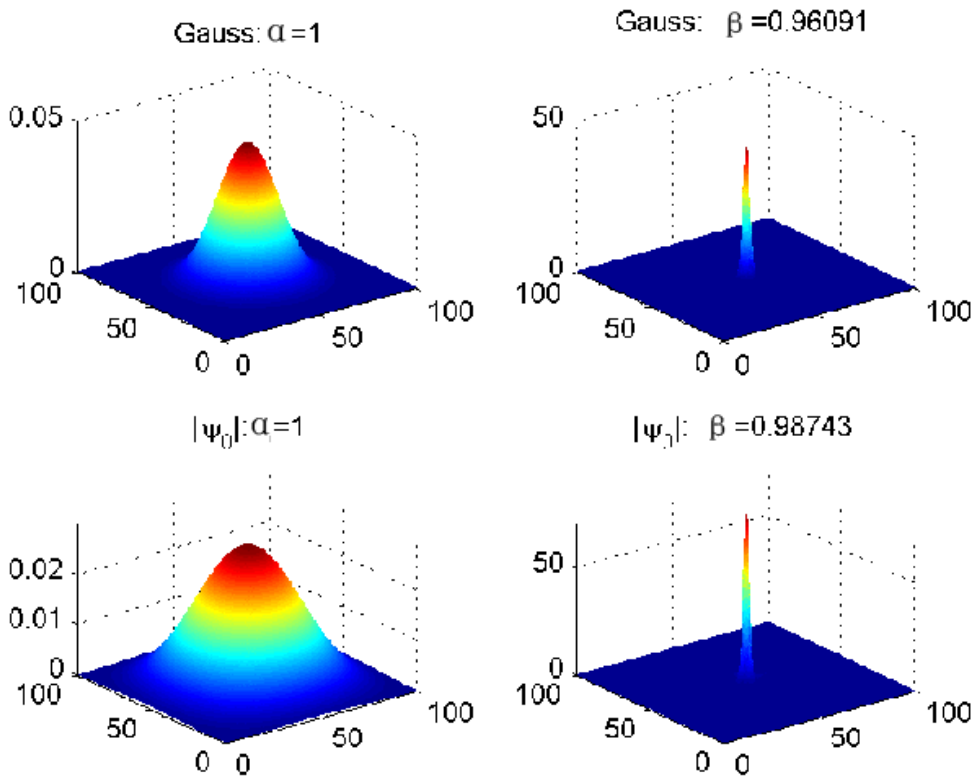

Figure 4: $\boldsymbol{\sigma}$-time-limited $\boldsymbol{g}(x,y)$ associated with QLCT and the modulus of $\psi_0(x,y)$ in time and QLCT-frequency domains with $a_1 = a_2 = 0.3$, $b_1 = b_2 = 1$, $c_1 = c_2 = -1$, $d_1 = d_2 = 0$.

6. Conclusion

This paper presented a new generalization of PSWFs, namely QPSWFs, which are the optimal $\mathbb{H}$-valued signals for the energy concentration problem associated with the QLCTs. We developed the definition of the QPSWFs associated with QLCTs and established various properties of them. In order to find the energy distribution of (α_f, β_f) for any $\mathbb{H}$-valued signals, we not only derive the Parseval identity associated with (two-sided) QLCTs, but also show that the maximum α_f for $\boldsymbol{\sigma}$-bandlimited signals associated with QLCTs in a fixed spatial domain must be QPSWFs.

Acknowledgments

The authors acknowledges financial support from the National Natural Science Foundation of China under Grant (No. 11401606,11501015), University of Macau (No. MYRG2015-00058-FST and No. MYRG099(Y1-L2)-FST13-KKI) and the Macao Science and Technology Development Fund (No. FDCT/094/2011/A and No. FDCT/099/2012/A3).

References

References

[1] J. A. Hogan and J. D. Lakey. *Duration and bandwidth limiting: Prolate Functions, Sampling, and Applications*. Springer Science and Business Media Press, 2011.

[2] A. Papoulis. *Signal analysis*. McGraw-Hill Press, 1977.

[3] C. Flammer. *Spheroidal Wave Functions*. Stanford University Press, 1957.

[4] W. J. Thompson. *Spheroidal wave functions*, Computing in Science and Engineering, 1(3), 84–87 (1999).

[5] D. Slepian and H. O. Pollak. *Prolate spheroidal wave functions, fourier analysis, and uncertainty–I*, Bell System Technical Journal, 40(1), 43–64 (1961).

[6] H. J. Landau and H. O. Pollak. *Prolate spheroidal wave functions, fourier analysis and uncertainty–II*, Bell System Technical Journal, 40(1), 65–84 (1961).

[7] H. J. Landau and H.O. Pollak. *Prolate spheroidal wave functions, fourier analysis and uncertainty–III: The dimension of space of essentially time- and bandlimited signals*, Bell System Technical Journal, 41(4), 1295–1336 (1962).

[8] D. Slepian. *Prolate spheroidal wave functions, fourier analysis and uncertainty–IV: Extensions to many dimensions; generalized prolate spheroidal functions*, Bell System Technical Journal, 43(6), 3009–3057 (1964).

[9] D. Slepian. *On bandwidth*, in Proceedings of the IEEE, 292–300 (1976).

[10] J. Kondo. *Integral equations*, Clarendon Press/Oxford University Press, 1992.

[11] Z. S. Michael. *The classical theory of integral equations a concise treatment*, New York: Birkhäuser Press, 2012.

[12] J. J. Ding and S. C. Pei. *Reducing sampling error by prolate spheroidal wave functions and fractional fourier transform*, in Proceedings of the IEEE International Conference on Acoustics, Speech, and Signal Processing, 217–220 (2005).

[13] H. Zhao, R. Wang, D. Song, and D. Wu. *Maximally concentrated sequences in both time and linear canonical transform domains*, Signal, Image and Video Processing, 8(5), 819–829 (2014).

[14] G. Walter and X. Shen. *Sampling with prolate spheroidal wave functions*, Sampling Theory in Signal Image Processing, 2, 25–52 (2003).

[15] G. Walter and X. Shen. *Wavelets based on prolate spheroidal wave functions*, Fourier Analysis and Applications, 10(1), 1–26 (2004).

[16] H. J. Landau and H. Widom. *Eigenvalue distribution of time and frequency limiting*, Mathematical Analysis and Applications, 77(2), 469–481 (1980).

[17] N. Tugbay and E. Panayirci. *Energy optimization of band-limited nyquist signals in the space domain*, IEEE Transactions on Communications, 35(4), 427–434 (1987).

[18] I. C. Moorea and M. Cada. *Prolate spheroidal wave functions, an introduction to the slepian series and its properties*, Applied and Computational Harmonic Analysis, 16(3), 208–230 (2004).

[19] S. Pei and J. Ding. *Generalized prolate spheroidal wave functions for optical finite fractional fourier and linear canonical transforms*, Optical Society of America A, 22(3), 460–474 (2005).

[20] T. Moumni and A. I. Zayed. *A generalization of the prolate spheroidal wave functions with applications to sampling*, Integral Transforms and Special Functions, 1–15 (2014).

[21] A. I. Zayed. *Generalized and fractional prolate spheroidal wave functions*, in Proceedings of the 10th International Conference on Sampling Theory and Applications, 268–270 (2014).

[22] H. Zhao, Q. Ran, J. Ma, and L. Tan. *Generalized prolate spheroidal wave functions associated with linear canonical transform*, IEEE Transactions on Signal Processing, 58(6), 3032–3041 (2010).

[23] G. Walter and T. Soleski. *A new friendly method of computing prolate spheroidal wave functions and wavelets*, Applied and Computational Harmonic Analysis, 19(3), 432–443 (2005).

[24] J. Morais, K. Kou, and Y. Zhang. *Generalized prolate spheroidal wave functions for offset linear canonical transform in clifford analysis*, Mathematical Methods in the Applied Sciences, 36(9), 1028–1041 (2013).

[25] A. Sudbery. *Quaternionic analysis*, Mathematical Proceedings of the Cambridge Philosophical Society, 85(2), 199–225 (1979).

[26] E. Hitzer. *Two-sided clifford fourier transform with two square roots of 1 in cl(p; q), advances in applied clifford algebras*, Advances in Applied Clifford Algebras, (2014).

[27] R. Ernst, G. Bodenhausen, and A. Wokaun. *Principles of Nuclear magnetic resonance in one and two dimensions*, Oxford University Press, 1987.

[28] E. B. Corrochano, N. Trujillo, and M. Naranjo. *Quaternion fourier descriptors for preprocessing and recognition of spoken words using images of spatiotemporal representations*, Mathematical Imaging and Vision, 28, 179–190 (2007).

[29] P. Bas, N. LeBihan, and J. M. Chassery. *Color image water marking using quaternion fourier transform*, in Proceedings of the IEEE International Conference on Acoustics, Speech and Signal Processing, 521–524 (2003).

[30] L. Chen, K. Kou, and M. Liu. *Pitt's inequatlity and the uncertainty principle associated with the quaternion fourier transform*, Mathematical Analysis and Applications, 423(1), 681–700 (2015).

[31] F. Brackx, R. Delanghe, and F. Sommen. *Clifford Analysis*, London: Pitman Research Notes in Mathematics, 1982.

[32] J. Morais, S. Georgiev, and W. Sprosig. *Real Quaternionic Calculus Handbook*, Birkhäuser, Basel Press, 2014.

[33] E. M. Hitzer. *Quaternion fourier transform on quaternion fields and generalizations*, Advances in Applied Clifford Algebras, 17(3), 497–517 (2007).

[34] S. A. Collins. *Lens-system Diffraction Integral Written in Terms of Matrix Optics*, J. Opt. Soc. Am., 60 1168-1177 (1970).

[35] M. Moshinsky and C. Quesne. *Linear cononical transforms and their unitary representations*, Mathematical Physics, 12, (1971).

[36] K. I. Kou, J. Ou and J. Morais. *Uncertainty principles associated with quaternionic linear canonical transforms*, Mathematical Methods in the Applied Sciences, 39, 2722-2736 (2015).

[37] X. Fan, K. I. Kou and M. Liu. *Quaternion wigner-ville distribution associated with the linear canonical transforms*, Preprint.

[38] D. Cheng, and K. I. Kou. *Properties of quaternion Fourier transforms*, Preprint.

[39] V. Anders. *Fourier analysis and its applications*, Springer Science and Business Media press, 2003.

[40] M. Bahri, R. Ashio, and R. Vaillancourt. *Convolution therorems for quaternion Fourier transform: properties and applications*, Abstract and Applied Analysis, 2013, 1–10 (2013).